"**Polynuclear Fe(II) Complexes: bi/trinuclear molecules, coordination networks**"

Jose Ramón Galán Mascarós,[a],[b] Guillem Aromí,[c],[d] and Mohanad Darawsheh[c]

[a] Institute of Chemical Research of Catalonia (ICIQ), The Barcelona Institute of Science and Technology (BIST), Av. Paisos Catalans, 16, 43007 Tarragona, (Spain). E-mail: jrgalan@ICIQ.ES
[b] ICREA, Pg. Lluís Companys 23, 08010 Barcelona, (Spain)
[c] Departament de Química Inorgànica i Orgànica; Universitat de Barcelona, Diagonal 645, 08028 Barcelona (Spain). E-mail:guillem.aromi@qi.ub.es
[d] Institue of Nanoscience and Nanotechnology of the University of Barcelona

ABSTRACT
In this manuscript, we review the recent progress made on the synthesis of Fe(II) coordination complexes with nuclearities two and three, as well as coordination polymers, that are relevant for their spin crossover (SCO) properties. The focus is put on the contributions made during the last five years. The structure of the compounds discussed is described as well as the main features of their magnetic properties. This manuscript is organized about the ligand types that serve to produce the various coordination systems presented, therefore, the structure of these organic donors are all gathered in various figures. The essential SCO parameters of all the compounds mentioned in the paper are summarized in a comprehensive table. This paper illustrates the richness and importance of the coordination chemistry that serves to advance the various facets of research on this fascinating phenomenon.

LIST of ABREVIATIONS

SCO	spin crossover
LS	low spin
HS	high spin
SCXRD	single crystal X-ray diffraction
SCSC	single crystal to single crystal
DMF	dimethylformamide
^{1}H-NMR	proton nuclear magnètic resonance
MS	mass spectrometry
CL	capping ligand
mer	meridional
fac	facial
LIESST	light induced excited spin state trapping
PB	Prussian blue
GM	guest molecule
e.g.	in latin, *exempli gratia* (for example)
salen	salicylaldehyde/ethylenediamine based ligand
abr.	abrupt
inc.	incomplete
gr.	gradual
2-st, 3-st	two and three steps, respectively
0D, 1D, 2D, 3D	zero, one, two and three dimensional, respectively

TABLE OF CONTENTS

1. Introduction

The phenomenon of spin crossover (SCO) confers the systems exhibiting this property the category of molecular switches. The reversible transitions between two spin states is accompanied by changes to the magnetic properties, but also to many other physical properties. In the case of Fe(II) (d^6), the SCO takes place between a diamagnetic spin state (S = 0; low spin, LS) and a paramagnetic spin

state (*S* = 2; high spin, HS).[1] Besides the dramatic impact on the magnetic behavior,[2] the transition may lead to radically different optical,[3-5] electrical[6-9] or chemical properties.[10-11] In addition, with Fe(II) the system experiences significant structural changes upon SCO. This is because the metal ion toggles between a HS state with two semi-occupied antibonding orbitals and a LS state with only occupied non-bonding orbitals. Therefore, the LS to HS transition causes an elongation of the coordination bonds to Fe(II) usually of 10-12%. Within a crystal lattice, these local structural effects propagate throughout the material and determine the dynamic properties of the transition; if the active SCO centers of the network are strongly connected by extended covalent or intermolecular interactions, the transition will likely be cooperative and may exhibit hysteresis and bistability.[12-13] In part for the above reasons, the vast majority of SCO systems studied are ferrous coordination compounds. It has become clear that complexes of Fe(II) with a majority of N-donors are prone to exhibit this behavior. While the number of reported systems is huge, the vast majority of SCO research performed in the areas of nano-structuration, advanced spectroscopic studies, guest-host research, etc. has focused on a reduced number of compounds, or families. This means that there is certainly a large amount of knowledge on the fundamentals and the potential of this phenomenon ready to be discovered from compounds already available. This shall be a consequence of the increased multidisciplinarity that is developing in recent years. In this review the focus is placed on the synthesis of SCO Fe(II) coordination compounds comprising active molecules of two or three metal centers, or coordination polymers, reported since 2012. Another paper of this special issue is consecrated already to mononuclear systems, while a third one focuses on non-ferrous systems. Clusters or polymers of Fe(II) with SCO behavior published previously to this year have been revised through excellent reviews.[14-18]

The special interest in polynuclear compounds is two-fold. On the one hand, polynuclear complexes are more prone to exhibit multi-step transitions, because of the easy implementation of crystallographically non-equivalent positions. This can be designed with the help of non-symmetric bridging ligands, for example. Multistep transitions could be the basis for developing multiple-state memories, beyond the simple binary system of <1> and <0> states. On the other hand, it is easy to envision how polynuclear compounds (and particularly coordination polymers) allow to establish stronger connectivity between SCO centers. Stronger connectivity typically means enhanced cooperativity, resulting in higher critical temperatures, more abrupt transitions, and appearance of wide hysteresis cycles. Indeed, most SCO materials with memory effect above room temperature are polynuclear complexes and coordination polymers.

The present paper is divided by nuclearities (from dinuclear to trinuclear to polymeric) and each block is organized by type of bridging ligands. A common feature of all the compounds reviewed in this manuscript is the presence of metals coordinatively linked by bridging ligands. All the bridging ligands have been named and their structures are shown through various figures. Very often, the assistance of additional capping ligands becomes necessary to complete the coordination sphere around the metals, and as helpful means to control/determine dimensionality. The latter are also listed. A list of all SCO

complexes featured in this review is given in a Table 1, where the main parameters of the magnetic behavior are indicated.

2. Recent Results

2.1 Dinuclear Complexes

Most discrete Fe(II) coordination compounds showing SCO are mononuclear.[19-21] These have been reviewed in some other part of this special issue. However, there has been an interest in preparing Fe(II) clusters exhibiting this property. On the one hand, this allows to probe, on simple systems, the synergy or correlation between SCO and intramolecular magnetic exchange.[22] In addition, they afford discrete molecules with more than two possible spin registries. In the case of dinuclear systems, these are [LS–LS], [LS–HS] and [HS–HS]. Experimental systems offer the possibility to study the interplay between these registries in comparison to the theoretical studies made on them.[23] In addition, dinuclear Fe(II) SCO molecules have shown the ability to tune the stability of the spin state at one site, via the structural consequences of the SCO on the other site.[24]

2.1.1 Complexes with 'N-N'- diazole bridges

Heterocyclic five or six membered rings containing the 'N-N'- diazole moiety are excellent bridging ligands, and are found profusely in coordination chemistry compounds (specially the former).[16, 25] Of particular relevance for the topic of SCO is the group of 1,2,4-triazoles (trz, Fig. 1), which give place to a largely studied family of Fe(II) complexes. Most triazoles lead to 1D coordination polymers with formula $[Fe(trz)_3]_n(X)_{2n}$ (X^- are counterions; see below),[18] however, a few discrete Fe/trz complexes have also been reported.[16, 26] One of the most interesting precedents is the complex $[Fe_2(L1)_5(NCS)_4]$ (**1**; L1, *N*-salicylidene-4-amino-1,2,4-triazole).[27] It features two Fe(II) centers bridged by three triazole ligands (L1) and bound to two additional capping L1 donors, with the coordination of each metal completed by two *cis* SCN^- groups. This compound exhibits abrupt SCO centered at $T_{1/2}$ = 150 K, as determined through magnetic measurements and confirmed by Mössbauer spectroscopy. The latter technique showed that the transition between the [LS–LS] and the [HS–HS] states occurs without the intermediacy of any [LS–HS] phase. Because of the photochromism of L1, complex **1** is fluorescent and the emission is very sensitive to the spin state, so that the SCO can be monitored through the luminescence of a probe that is well separated from the metal centers. To the publication of **1** followed reports on a few other derivatives. The structure of the complex $[Fe_2(L2)_5(NCS)_4]$ (**2**, Fig. 2; L2, 4-phenylimino-1,2,4-triazole)[28] is completely analogous to **1**. It features the SCO of approximately half of its metal centers with a $T_{1/2}$ value of 115K. The analysis of the molecular structure **2** at 100K reveals that each Fe(II) center of the molecule exhibits parameters half way between the LS and the HS states, thus suggesting that, at this temperature, the lattice does not contain ordered [LS-HS] entities. Therefore, the mixed-spin system, containing [HS–HS] entities at low temperature, offered the possibility to probe for the first time the intramolecular antiferromagnetic interaction between both metals. If crystals of **2** are left in air, they turn into powder following the exchange of lattice methanol molecules by water. This changes the spin state of **2** into [HS-HS] for the whole range of temperatures and confirms the intramolecular antiferromagnetic coupling. A similar solvent effect was observed on the analogue $[Fe_2(L3)_5(NCS)_4]$ (**3**; L3, 4-(2-pyridyl)-1,2,4-triazole).[29] Interestingly, two solvatomorphs could be prepared independently by using, respectively, MeOH/EtOH and water as solvents and the products were perfectly characterized

by single crystal X-ray diffraction (SCXRD). The former incorporates molecules of MeOH and EtOH in the lattice and exhibits a SCO of 50% of the metal centers. The other derivative features water lattice molecules and 100% of its iron centers are in the HS state down to 2K. The interesting difference with **2** is that the low temperature phase of the mixed-spin compound is now made of ordered [LS-HS] molecules. This behavior was confirmed thoroughly on the new derivative $[Fe_2(L4)_5(NCS)_4]$ (**4**; L4, 4-phenyl-1,2,4-triazole).[30] The MeOH·EtOH solvate exhibits the same structural features and magnetic behavior as its analogue with **3**. The preparation of **4** in ethanol affords the EtOH solvate, also undergoing SCO of 50% of its iron centers. This solvate exhibits in the atmosphere a single crystal to single crystal (SCSC) transformation described as **4**·2EtOH + 1.5 H_2O → **4**·2EtOH·1.5H_2O. As an attempt to correlate the SCO properties with the electronic properties of ligand substituents, the 2,5-dichloro version of L2 (*i.e.* 2,5-dichloro-4-phenylimino-1,2,4-triazole; L5) was employed to make the complex $[Fe_2(L5)_5(NCS)_4]$ (**5**). Its H_2O solvate was found to exhibit complete SCO with a $T_{1/2}$ 35 K higher (at 150 K).[31] This shift is attributed, in part to a larger electron withdrawing capacity of the substituents, although there could be other effects playing a role.

One strategy for enforcing the formation of discrete dinuclear molecules with 'N–N' bridges from triazole or pyrazole moieties is by incorporating to these rings substituents with donor atoms also capable of coordinating the metals. These ligands, together with XCN^- anions (X=S, Se or BH_3) furnish a suitable recipe for the preparation of SCO complexes.[14] The early examples where made of 3-(2'-pyridyl)-pyrazole (L6)[32] and 3,5-*bis*-(2'-pyridyl)-pyrazole (L7),[33] and served, for example, to characterize for the first time an ordered phase with two components, the [LS–LS] and the [LS-HS], at the intermediate plateau of a two-step SCO.[34] In addition, thanks to the synthetic versatility allowing to change the neutral terminal ligands that complete the coordination sphere of the metal ions, this family of compounds was used to probe the tunability of the SCO temperature as a function of this ligand.[35] One of these compounds, $[Fe_2(NCSe)_2(L7)_2(py)_2]$ (**6**)[36] was used to establish a relationship between the lattice at the atomic level and the macroscopic orientation of the LS-HS interface during the thermal transition. It was found that the orientation of this interface is that causing the least mismatch between both phases at the nanoscale.[37] The above dinuclear compounds and these made with the triazole analogue 3,5-*bis*-(2'-pyridyl)-1,2,4-triazole (L8)[36] have constituted a suitable basis to calculate whether the transition between the [HS–HS] and the [LS–LS] state shall occur directly or through the formation of an ordered phase of the intermediate [LS–HS] component.[38] Very recently, the related asymmetric ligand 3-(2'-pyridyl)-4-(*p*-tolyl)-5-(3'-pyridazine)-1,2,4-triazole (L9) was used to prepare the analogous dinuclear complex $[Fe_2(L9)_2(MeCN)_4](BF_4)_4$ (**7**).[39] The lattice of this molecule was shown to undergo various solvent exchange processes as SCSC transformations, which were accompanied by changes to the spin state of the Fe(II) ions and therefore, of color. These phenomena convert this system into a candidate of molecular chemical sensor of small molecules or gases.[40] Thus, exposure of **7** to EtOH transforms it into $[Fe_2(L9)_2(EtOH)_4](BF_4)_4$ (**8**) while the process can be reversed by passing vapors of MeCN on **8**. The latter compound is in turn converted to $[Fe_2(L9)_2(H_2O)_4](BF_4)_4$ (**9**) employing H_2O in the gas phase. One remarkable thing is that **9** is in fact polymeric, and forms as a result of a change in coordination mode of L9, which turns from μ into μ_3 by rotation of the

pyridazine group. The polymerization is reversible by dehydration through heating, followed by exposure to an MeCN atmosphere.

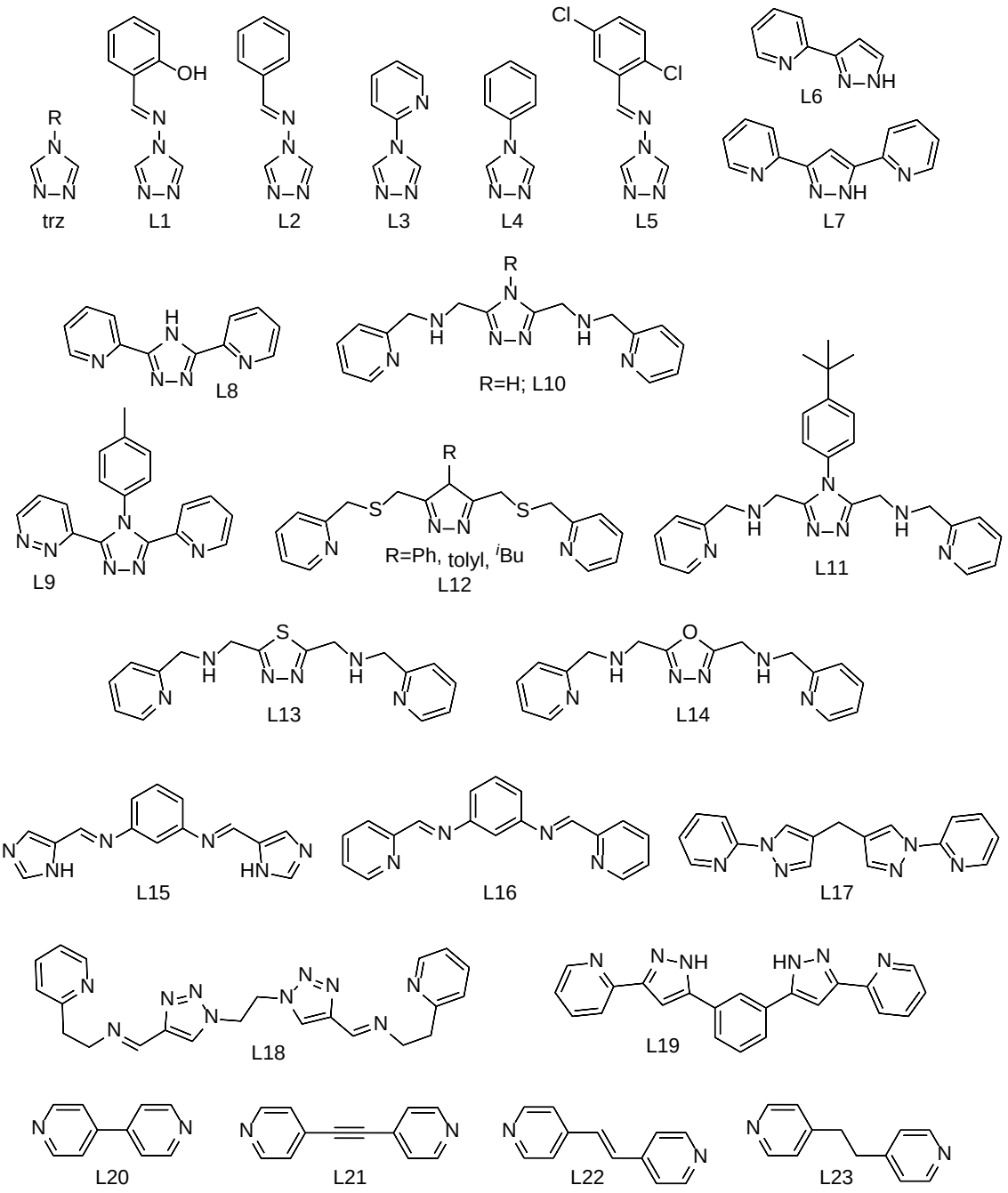

Figure 1. Structure of bridging ligands mentioned in this review.

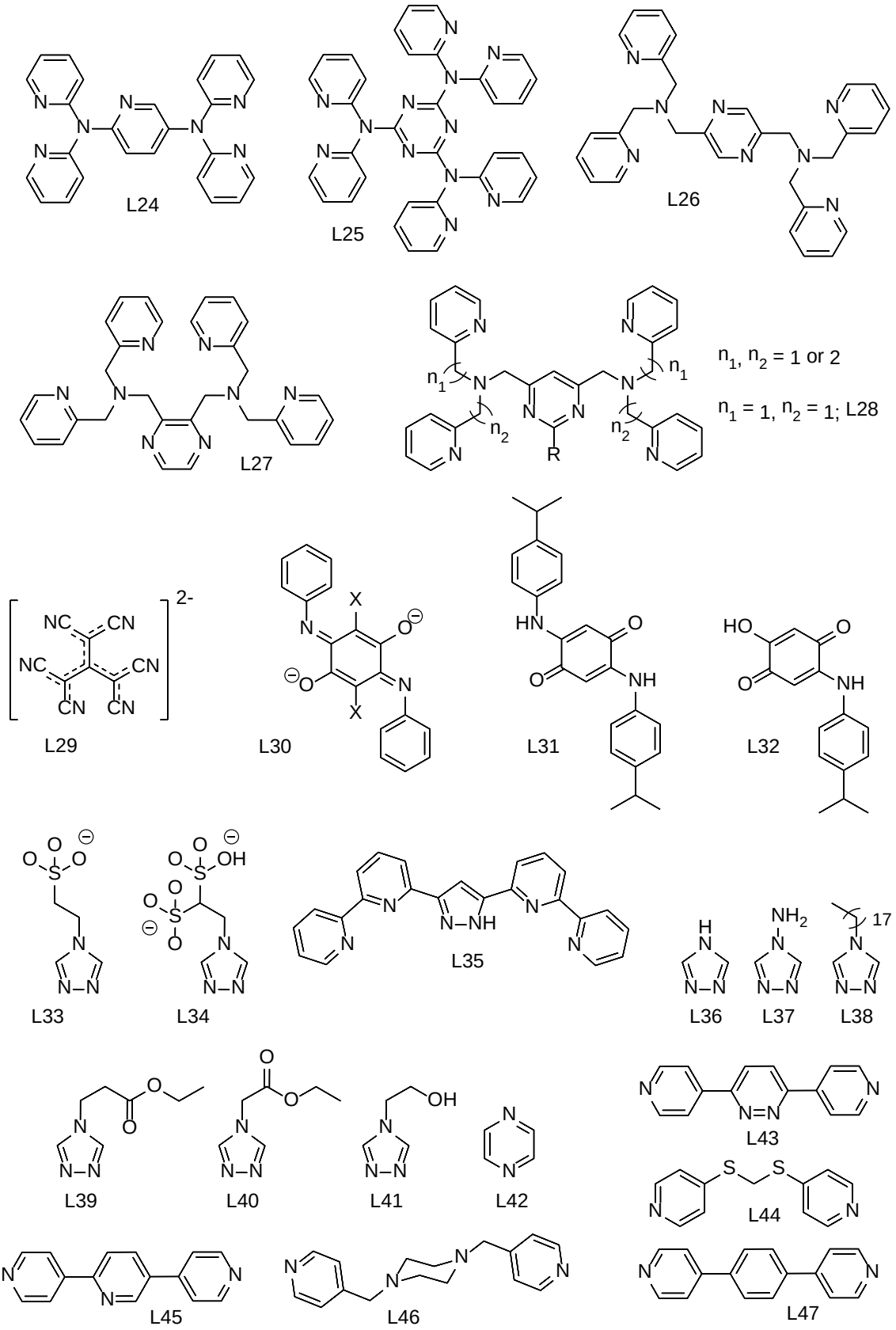

Figure 1 (continued I). Structure of bridging ligands mentioned in this review.

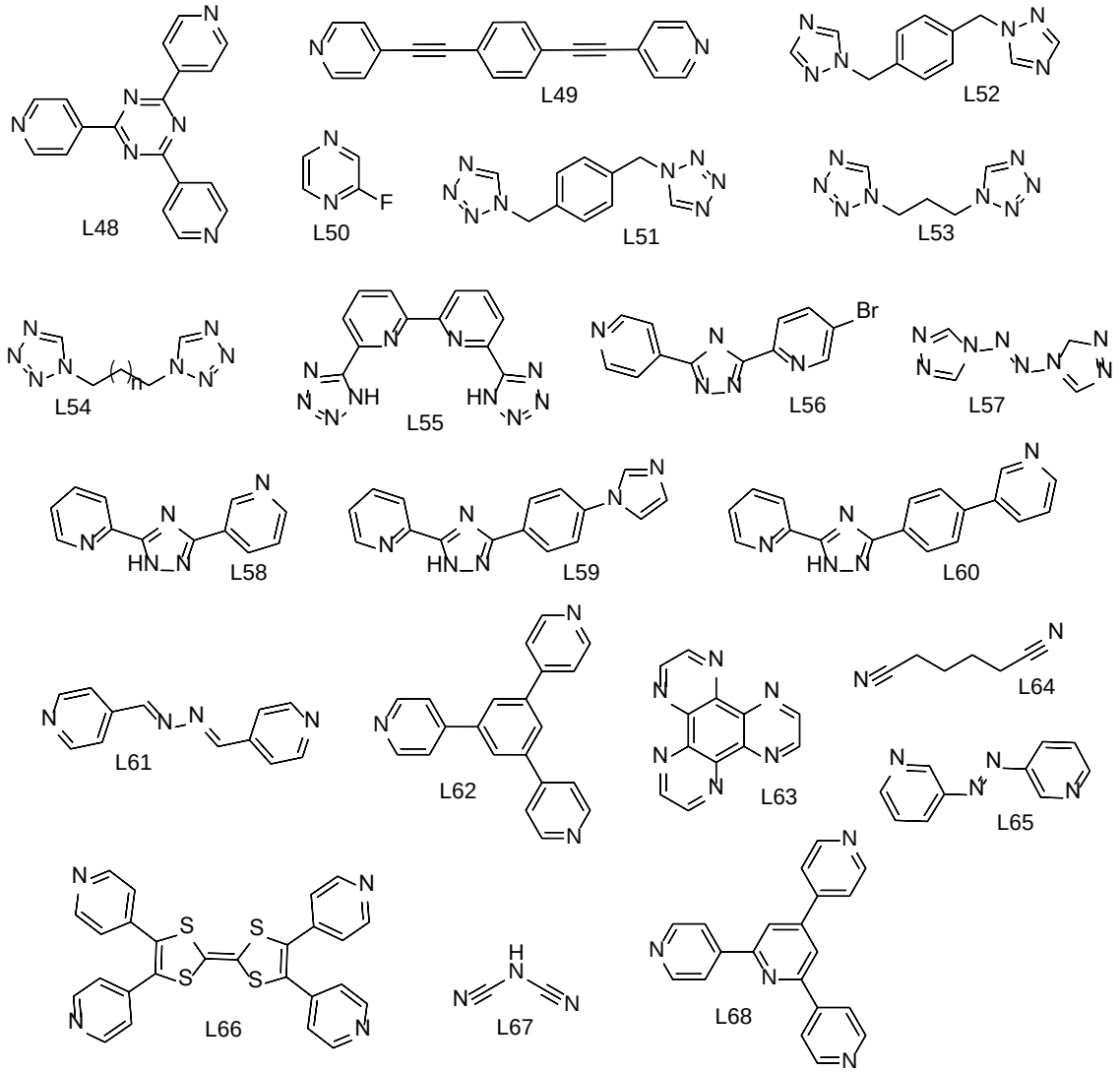

Figure 1 (continued II). Structure of bridging ligands mentioned in this review.

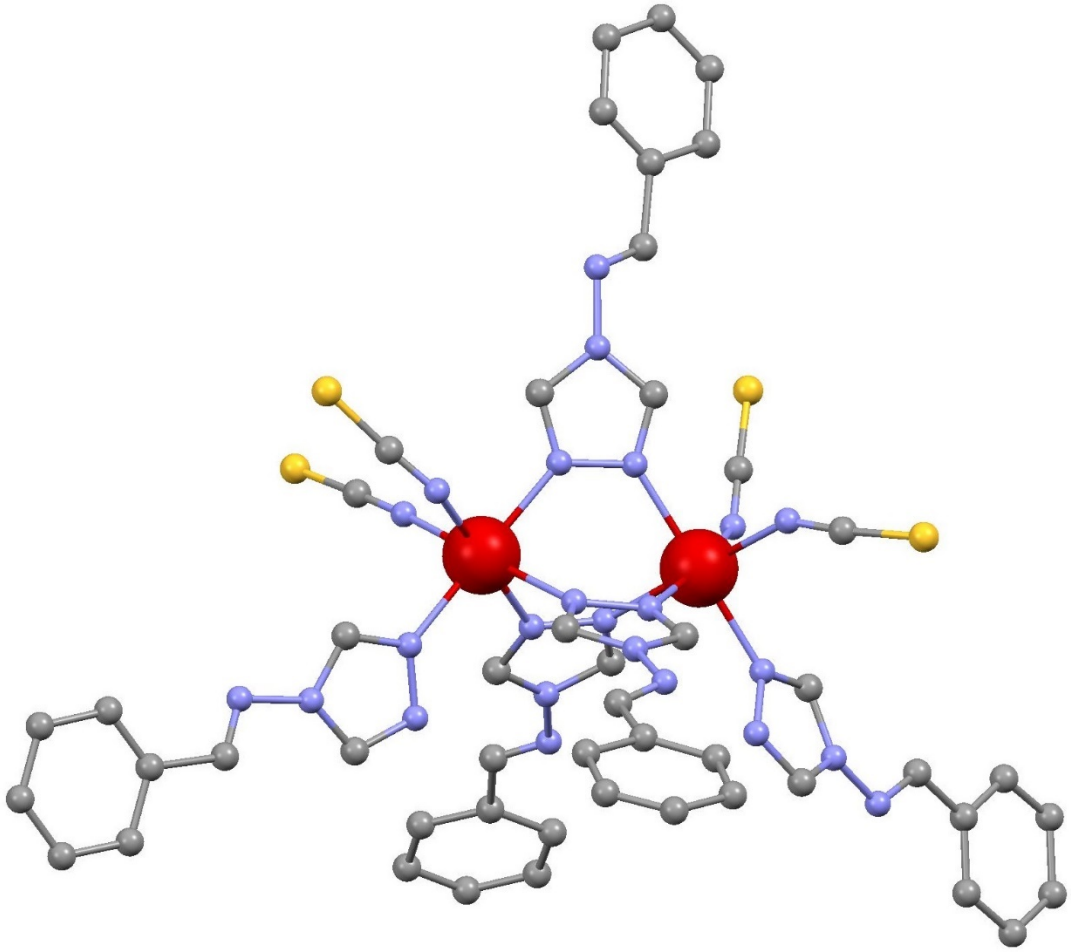

Figure 2. Molecular structure of $[Fe_2(L2)_5(NCS)_4]$ (**2**).[28] Color guide; Fe (LS), red; C, grey; N, purple; S, yellow. H-atoms not shown.

A set of ligands related to L8 and L9 are these derived from 3,5-bis-(((2-pyridylmethyl)-amino)-methyl)-4*H*-1,2,4-triazole (L10), which bear one additional nitrogen donor moiety at each side of the triazole, appropriately disposed to yield dinuclear complex cations, $[Fe_2(L10)]^{4+}$ (**10**), similar to **6** – **9**, while coordinatively saturating both Fe centers. Such molecules are prone to exhibit SCO properties with relative independence of the counter-ion identity, since the latter would not act as ligand. The differences caused by solvation effects and lack of structural information for the whole series prevented to extract a general picture on the SCO behavior.[41] Following a commendable effort in synthetic organic chemistry, a large series of derivatives of L10 was prepared with various substituents at position 4 of the central tetrazole. This lead to an investigation of the effect of this substituent on the SCO. The behavior observed consisted on complete, gradual [HS-HS] to [HS-LS] transitions upon cooling from room temperature or on the persistence of the HS state in both metals. It was concluded that the differences were rather attributed to packing effects.[42] One such complex, $[Fe_2(L11)](BF_4)_4$ (**11**; L11, 3,5-bis-(((2-pyridylmethyl)-amino)-methyl)-4-(*p*-tertbutylphenyl)-1,2,4-triazole, Fig. 3), was found to exhibit abrupt SCO between the [LS–HS] and the [HS–HS] states with a 22 K wide hysteresis loop.[24] A scan rate dependence of

this loop showed that the experiment dynamics only affects the position of the cooling branch, making the loop wider upon slowing the decrease of the temperature. In a very interesting development with this kind of ligands, a similar family of compounds of the parent ligand 3,5-*bis*-(((2-pyridylmethyl)-sulfanyl)-methyl)-4H-1,2,4-triazole (L12) was created.[43] This set of donors was employed to investigate anew the effect of the substituents on the SCO properties of the Fe_2 complexes of the type $[Fe_2(L12)]^{4+}$ (**12**), that predictably would form, in this occasion featuring N_4S_2 coordination environments around the metals. This study is of interest since Fe(II) complexes exhibiting this environment and spin transition behavior are very scarce. It unveiled a variety of SCO properties, including the observation of the [LS-LS] state in some of the derivatives, and also revealed that the tendencies observed in the solid state are opposite to these seen in solution. Thus, the SCO in the solid state is dominated by packing effects whereas the σ-donating ability of the triazole substituent dominates the SCO temperature in solution. Another variation in this category of ligands is changing the nature of the central heterocycle. Thus, ligand 2,5-*bis*-((2-pyridylmethyl)-amino)-methyl-1,3,4-thiadiazole (L13) combines with the bridging N–N diazole in this ring an atom of sulfur.[43] This leads undoubtedly to changes to the electronic environment around the metals and, according to the authors, also provides a higher flexibility in the coordination geometry. The result of this is that with (L13) the corresponding $[Fe_2(L13)]^{4+}$ (**13**) cations have a much more marked tendency to remain in the [LS-LS] state, only starting to undergo thermal SCO from 250 K or higher temperatures. This family of compounds was used to illustrate the crucial influence of the lattice solvent molecules on their solid-state magnetic properties.[44] Thus, while the complex **13**$(BF_4)_4$·4DMF is in the [LS–LS] state up to 300 K, the product resulting from thermally removing the solvent molecules becomes [HS–HS] near room temperature and then experiences a SCO to the [LS–HS] state at 280K. This radically distinct behavior is reversed back to the original one by exposing the solid to an atmosphere of DMF. This process of solvent desorption/adsorption can be repeated over several cycles, with the consequent changes to the magnetic properties. In view of these interesting results this research was extended to the ligand 2,5-*bis*-((2-pyridylmethyl)-amino)-methyl-1,3,4-oxadiazole (L14), which compared with L13, bears an oxygen atom instead of a sulfur atom on the central diazole ring.[45] Changing the counter anion within the set of compounds $[Fe_2(L14)]X_4$ (**14**) led to dramatically distinct SCO properties ranging from [HS-HS] in the whole temperature range studied ($X=BF_4^-$), a SCO from [HS-HS] to [LS-HS] centered near 147 K ($X=ClO_4^-$) to a similar spin transition with a 26 K wide hysteresis. This is a very rare case of hysteresis of a polynuclear SCO complex.

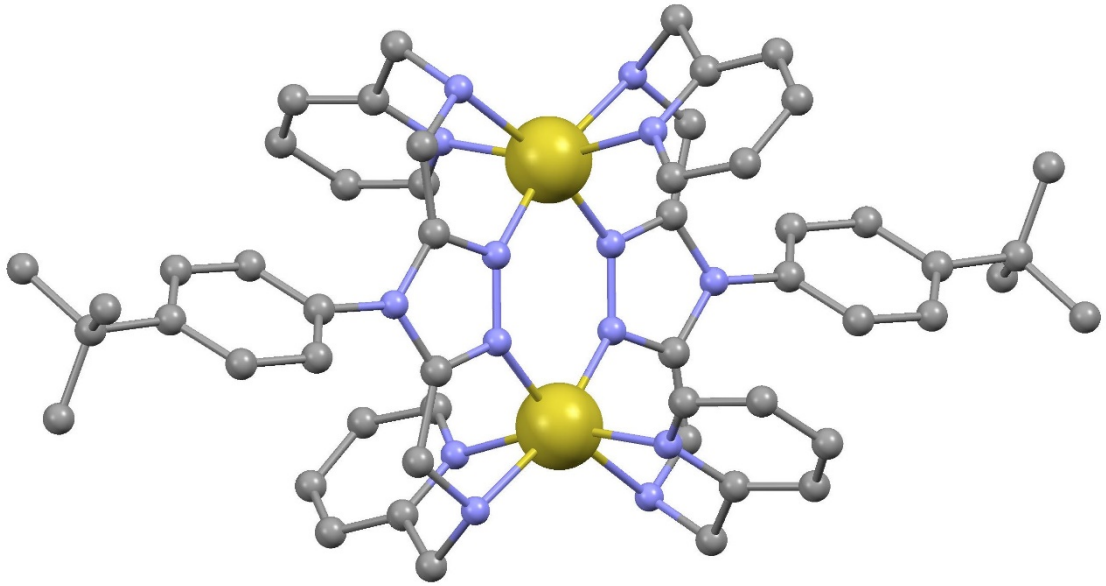

Figure 3. Molecular structure of $[Fe_2(L11)](BF_4)_4$ (**11**).[24] Color guide; Fe (HS), yellow; C, grey; N, purple. H-atoms not shown.

2.1.2 Triple stranded helicates or mesocates

Of the large family of coordination supramolecular helicates,[46-47] very few have been exploited in the context of SCO. Here, helicates are coordination complexes of two or more metals contained in the axis of the helix, coordinated by bridging ligands constituting the strands. In the case of dinuclear systems, if the chirality at the metal centers are different, the molecules constitute mesocates (they are identical to their mirror image). Among the earliest precedents is a family of Fe(II) dinuclear triple-stranded helicates made of bis-methyleneimineimidazole moieties. These helicates exhibit spin transitions from the [HS–HS] states at room temperature, of varying completeness and temperature, depending on the nature of the counter-ion (*i.e.* PF_6^-, BF_4^- or ClO_4^-),[48] while a related helicate with a very similar ligand showed marked changes to the magnetic properties as a result of thermal desolvation and a very rich photomagnetic behavior.[49] Much more recently, an analogous ligand, comprising a shorter spacer (N,N′-bis(1Himidazol-4-ylmethylene)benzene-1,3-diamine, L15), was shown to impose a strain within the molecular ensemble, causing the formation of a *mesocate* ($[Fe_2(L15)_3](BF_4)_4$), **15**) rather than a helicate, with fixed Fe–N distances that force the [HS-HS] state down to 2K.[50] The equivalent to L15 with pyridyl, rather that imidazolyl (N,N′-bis(pyridine-2-ylmethylene)benzene-1,3-diamine, L16) exerts the same effects, producing the corresponding mesocate $[Fe_2(L16)_3](BF_4)_4$ (**16**), which exhibits a SCO at 350 K, contrary to what is expected for pyridylimine Fe(II) tris-chelates, usually found in the LS state. A similar ligand featuring two connected 1-(2-pyridyl)pyrazoles instead of imidazolimines (4,4'-(methylene)-bis-(1-(2-pyridyl)pyrazole, L17) also yields the expected helicate, $[Fe_2(L17)_3](BF_4)_4$ (**17**).[51] This complex was characterized by SCXRD and also in solution, *via* ^{1}H-NMR and mass spectrometry (MS). All the experiments confirmed the [LS–LS] state of the metals at all temperatures.

The ligand 1,1′-(1,2-ethanediyl)-bis-1,2,3-triazol-4-yl-methylideneamino-2-ethylpyridine (L18) comprises two tridentate 'N,N,N' coordination pockets separated by a flexible spacer.[52] This confers this donor the ability to form double

stranded (instead of triple stranded) dinuclear helicates around six-coordinate metal ions. The complex formed by reaction with $Fe(PF_6)_2$, $[Fe_2(L18)_2](PF_6)_4$ (**18**), falls under this definition. It shows a gradual and incomplete SCO starting from the low temperature [LS-LS] state, before it continues in a very abrupt manner to a complete [HS-HS] state. The sudden change of dynamics starts in fact before reaching 50% conversion of the Fe centers, it is reversible and yields an 11 K wide hysteresis. No other helicates featuring hysteresis have been reported so far.

The possibility of preparing SCO supramolecular helicates offers the possibility of exploiting their potential to encapsulate functional guests as a way to combine magnetic switching abilities with other properties. This, shall be done using the cavity available at the center of the assembly by benefiting from its internal symmetry and its ability to establish supramolecular interactions with guests. Ligand 1,3-bis[1-(pyridine-2-yl)-pyrazol-3-yl]benzene (L19) exhibits two imidazolylpyridine chelating units, known to confer SCO properties to Fe(II),[53] separated by a phenylene spacer.[54] The N–H moieties of the pyrazolyl fragments point towards the interior of the cavity of the helicate formed upon coordination with Fe(II), becoming thus poised for their interaction through hydrogen bonds with guests acting as acceptors. This cavity is well suited for fixing Cl^- and Br^- anions. Thus, the composite supramolecular ensembles $X@[Fe_2(L19)_3]X(PF_6)_2$ (X=Cl, **19**; Br, **20**, Fig. 4) were prepared and characterized. SCXRD and magnetic measurements show that **19** and **20** exhibit ordered [LS–HS] mixed-spin molecules that change thermally to [HS-HS]. The guest serves to tune the SCO temperature, which is shifted by 40 K (from 265 to 305 K in going from Br^- to Cl^-). The SCO of one of the metal ions of the $X@[Fe_2(L19)_3]^{3+}$ entities can be followed by monitoring the variation of the average Fe–N distances with temperature *via* SCXRD while the other metal center maintains constant parameters (Fig. 4). Interestingly, **19** and **20** experience SCSC transformations upon exposure to air, by exchange of some lattice MeOH molecules by H_2O. The resulting solvatomorphs experience a two-step (**19**, Cl) or a gradual (**20**, Br) SCO from the [HS–HS] to the [LS-LS] in passing through the [LS–HS] species. The three states of these hydrates were also characterized by SCXRD. ^1H NMR and MS demonstrated the persistence of these inclusion helicates in solution, together with small amounts of the guest free species, as well as of a supramolecular assembly resulting from the recognition of two mononuclear $[Fe(L19)_3]^{2+}$ units entangled together with a central X^- (Cl or Br) anion. The latter could be subsequently isolated under the appropriate experimental conditions and characterized.[55]

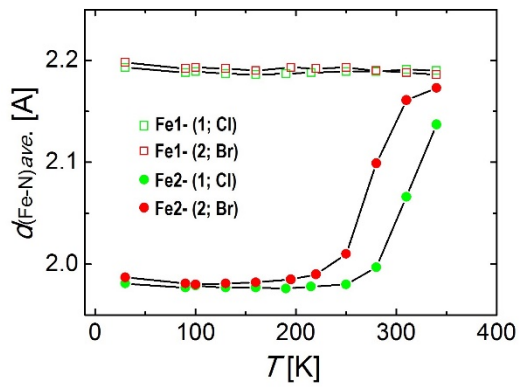

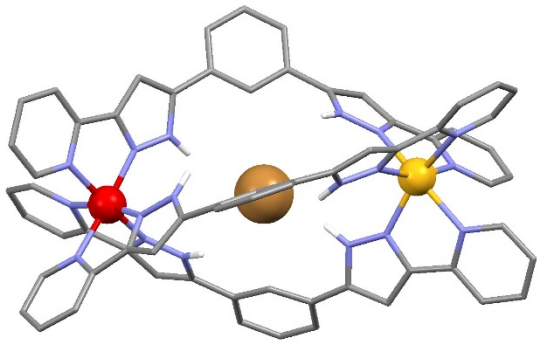

Figure 4. (left) Temperature dependence of the average Fe–N distances for compound Br@[Fe_2(L19)$_3$]Br(PF_6)$_2$ (**20**) as determined through single crystal X-ray diffraction and (left) molecular structure of this compound.[54] Color guide; Fe (LS), red; Fe (HS), yellow; C, grey; N, purple; H, white. Only H-atoms of N-H groups shown.

2.1.3 Complexes with 4,4'-dipyridyl-type ligands

A useful approach to prepare multinuclear SCO compounds is by linking preformed coordinatively unsaturated coordination complexes with the appropriate bridging ligands. Complexes possessing labile, easy to substitute ligands are also suitable building blocks. Poly-pyridyl ligands are perhaps the most popular bridging ligands in this area of supramolecular coordination chemistry.[56-59] In the context of Fe(II) SCO, the first dinuclear complexes made in this way incorporated 4,4'-bipyridine (L20) as bridging ligand.[60] Complex [Fe_2($NCS)_4$(CL1)$_2$(L20)] (**21**; CL1, 2,6-*bis*-(3-pyrazolyl)-pyridine, Figure 5) features two equivalent, separated Fe(II) building blocks within a molecule, each containing two *trans*-NCS^- terminal ligands in addition to a *meridional* (*mer*) capping ligand (CL1; 2,6-*bis*-(pyrazol-3-yl)-pyridine). It exhibits [LS–HS] to [HS–HS] SCO and this transition can also be triggered by light irradiation through the light induced excited spin state trapping (LIESST) effect. Changing the capping ligand from CL1 to di(2-picolyl)amine (CL2) leads to the analogous complex [Fe_2($NCS)_4$(CL2)$_2$(L20)] (**22**).[61] Since the capping ligand is now *facial* (*fac*), the NCS^- ligands in **22** are *cis*. This complex exhibits a full transition from [HS–HS] to [LS–LS], passing through a recognizable phase composed of [LS–HS] species. The related bridging ligand 4,4′-dipyridylethyne (L21) was employed in combination with the N_2O_2 Shiff base donor CL3. Since the latter imposes the occupation of four equatorial positions around a metal center in a square geometry, the only two remaining sites for octahedral coordination are *trans* axial. This favors, in combination with linear bridging ligands, the formation of 1D coordination polymers (see below). Discrete dinuclear complexes could be obtained capping both ends with solvent terminal ligands, leading to [Fe_2(CL3)$_2$(L21)(ROH)$_2$] (**23**, R=Me or Et).[62] The nature of the donor atoms around the Fe(II) centers, N_3O_3, favors a HS state, which is observed with these compounds at all temperatures. The metathesis of these terminal ligands by N-based terminal ligands would perhaps confer SCO properties to the assembly. Subsequent synthetic work was conducted in order to draw structure/property correlations. This was done by changing the nature of the bridging ligand while maintaining the rest of the molecular structure intact within complexes of the type [Fe_2($NCS)_4$(CL2)$_2$(L)] (eg. L=L20, **22**; L22, 4,4′-dipyridylethene, **24**). These studies revealed that simply comparing solvatomorphs or even polymorphs of the same compound yields completely different magnetic properties.[63] Analysis of the magnetic properties of several solvates and polymorphs of, eg. **22** and **24** in light of their SCXRD structures revealed that the SCO properties were mostly related to the local distortion around the FeN_6 coordination polyhedron, rather than to the electronic or structural properties of the bridging ligands.[64] These distortions are in turn related to the packing of the molecules within the crystal lattice. This study was completed with the synthesis of a new family of compounds, this time featuring a new terminal ligand; $NCBH_3^-$. The new group of compounds, [Fe_2($NCBH_3)_4$(CL2)$_2$(L)] (L=L20, **25**; L21, **26**; L23, 4,4′-

dipyridylethane, **27**) served to confirm elegantly the conclusions extracted from the previous investigation.[65]

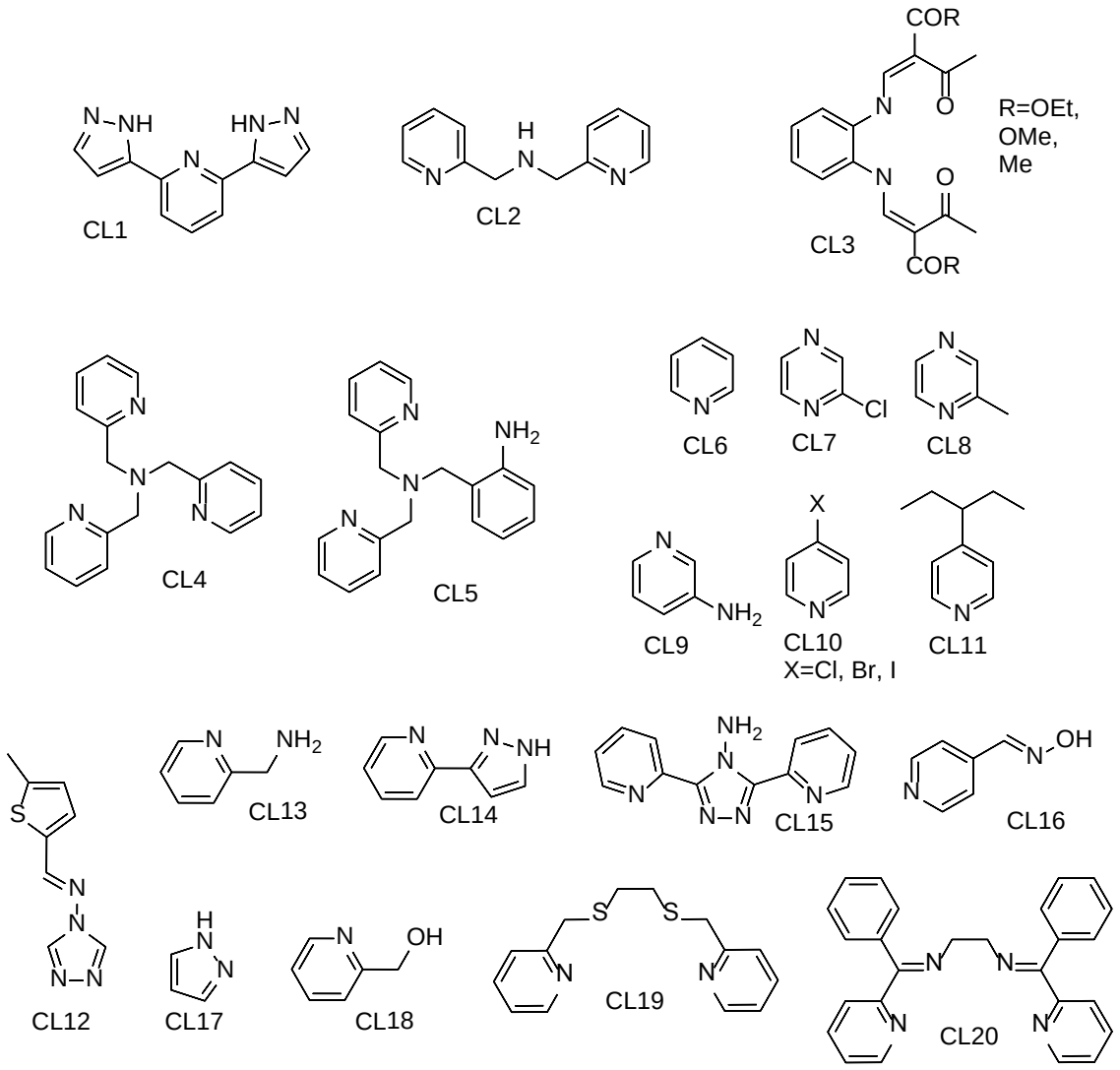

Figure 5. Structure of capping ligands mentioned in this review.

2.1.4 Complexes with poly-dipyridyl-type ligands

The evidence that pyridyl donor groups favor the manifestation of SCO properties upon coordination to Fe(II) centers motivates the synthesis of ligands incorporating several such groups. Some of these are designed to act as bridging ligands, as an extension of the *bis*-pyridine species of the previous section. One of the significant early precedents was the complex $[Fe_2(L24)_2(NCS)_4]\cdot$(**28**; L24, 2,5-bis-(2',2''-dipyridylamino)pyridine). It was a remarkable contribution since it exhibits a two-step full SCO, involving transitions between the three states [LS–LS], [LS–HS] and [HS–HS], which were all characterized by SCXRD, for the first time in a dinuclear Fe(II) system.[66] This compound, prepared as a solvate with four molecules of CH_2Cl_2 molecules per complex, exhibits remarkable partial or total desolvation effects, which are reversible and are accompanied by drastic changes to the magnetic properties. The dependence of these properties as a function of the degree of solvation with CH_2Cl_2 or $CHCl_3$ as well as their capacity to undergo LIESST effect were reported in a subsequent paper.[67]

A related ligand comprising three chelating units, 2,4,6-tris-(2',2''-dipyridylamino)-1,3,5-triazine (L25), had also been employed to obtain dinuclear Fe(II) complexes.[68] With complexes $[Fe_2(L25)(H_2O)_2S_2]X_2$ (S, X = MeOH, ClO_4^-, **29**; MeCN, BF_4^-, **30**), it was shown that the nature of the solvate ligand influences dramatically the magnetic properties, in going from a SCO system (**29**) to a fully HS complex at all temperatures (**30**). Another complex featuring Fe–N bonds with the central triazine of L25 was also obtained, $[Fe_2(L25)Cl_2](CF_3SO_3)_2$ (**31**). This compound is in the [HS–HS] state down to low temperature, where the onset of very unusual ferromagnetic coupling is detected.

More recently, the synthesis of two new polypyridyl ligands has been reported; 2,5-bis-(N,N-bis-(2-pyridylmethyl)aminomethyl)-pyrazine (L26) and 2,3-bis-(N,N-bis-(2-pyridylmethyl)aminomethyl)-pyrazine (L27).[69] These ligands possess up to eight N-donor atoms and they react with Fe(II) to form dinuclear complexes engaging all these hydrogen atoms, thus acting as bis-tetradentate donors. The resulting complexes, $[Fe_2(L26)_2(NCS)_2]$ (**32**) and $[Fe_2(L27)_2(NCS)_2]$ (**33**), show very gradual SCO to the [HS–HS] state, starting from an intermediate and from a quasi-pure [LS–LS] state, respectively. Upon desolvation at 400 K (by loss of one molecule of DMF and two molecules of H_2O), complex **32** experiences a marked change of behavior, then exhibiting an extremely abrupt SCO with a small hysteresis (and $T_{1/2}$ values of 184 and 189 K). Dessolvated **32** and complex **33** were irradiated at low temperature with light of 532 nm, both systems showing a rapid transition to metastable [HS–HS] states. In both cases, this transition unveils the existence of intramolecular antiferromagnetic interactions. Three ligands very related to L26 and L27 were prepared in order to extend further this investigation. These are derivatives of L28 (4,6-bis-(N,N-bis-(2-pyridylmethyl)aminomethyl]-2-phenylpyrimidine), an comprise a central pyrimidine (instead of pyrazine).[70] The difference is that half or all of the methylpyridine arms are replaced by ethylpyridine. In all cases, complexes analogous to $[Fe_2(SCN)_4(L28)_2]$ (**34**) were prepared, where the NCS^- ligand could also be replaced by $NCSe^-$ or $NCBH_3^-$. Interestingly, unlike with the previous examples, all these compounds were found in the [HS–HS] state at all temperatures. The authors of this study suggest that the weaker field furnished by the pyrimidine central ring is the reason of this magnetic behavior. They also mention that the distortion of the coordination geometry around the metal centers is significantly distorted. This could also be the reason for the spin state observed in this family of compounds.

2.1.5 Complexes with other types of bridging ligands

A few other bridging ligands have been used recently to form dinuclear Fe(II) molecules with SCO properties. One such bridging ligand is the cyanocarbanion L29 (2-dicyanomethylene-1,1,3,3-tetracyanopropanediide dianion).[71] The use of flexible tetradentate capping ligands CL4 (tris(2-pyridylmethyl)amine) and CL5 (bis(2-pyridylmethyl)-(2-anilylmethyl)amine) leave two remaining sites on Fe(II), featuring a *cis* configuration, in perfect disposition for the binding of two L29 ligands and the formation of dinuclear complexes $[Fe_2(L29)_2(CL4)_2]$ (**35**) and $[Fe_2(L29)_2(CL5)_2]$ (**36**). Both complexes exhibit SCO, with very different transition temperatures (more than 170 K of difference). In fact, compound **35** is obtained as a MeOH solvate (one methanol molecule per complex) however, it loses this solvent in contact with air. Therefore, it is not possible to know if the original solvate has SCO since the solvent desorption occurs before any transition is

observed. The measured [LS] to [HS] transition corresponds to that of the dessolvated species. The SCO of complex **36** is not superimposable in the cooling and warming branch, presumably also because of solvent desorption. However, the latter occurs near room temperature, after the SCO of the solvate.
The ligand 2,5-dianilino-1,4-benzoquinone (L30) was prepared with various substituents 'X' at positions '3' and '6' (X=H, F, Cl, Br, I) in order to study the electronic effects on the SCO properties of dinuclear complexes $[Fe_2(L30)(CL4)_2](TFPB)_2$ (**37**) and the derivatives, prepared by design, using CL4 as capping ligand (as in the previous complexes) and the bulky anion tetrakis-(3,5-bis(trifluoromethyl)phenyl)borate (TFPB).[72] The five derivatives experience a one-step incomplete SCO from a mixture of HS/LS state to the [HS-HS] state. There is a correlation between $T_{1/2}$ and the substituent with the following order; H > Br > Cl > F. The percentage of HS Fe centers remaining at low temperature follows the inverse order, consistent with larger stabilization of the HS by a more electronegative substituent. If the temperature is decreased further, the magnetization measurements indicate the existence of ferromagnetic interactions between HS Fe(II) centers, with responses that become more important as the percentage of HS species is larger. This indicates that the mixed spin state is formed by [LS–HS] and residual [HS–HS] with no presence of [LS–LS] molecules. Quantitatively, the magnetic susceptibility curves are consistent with this hypothesis. The latter was corroborated by Mössbauer spectroscopy, which probed the presence of either only one type of HS Fe(II) for the [HS-HS] (high temperature), or in addition, upon reduction of the temperature, of the presence of two new doublets for the Fe centers in the [LS–HS] species.
Ligands L31 (double deprotonated 2,5-bis-(4-(isopropyl)anilino)-1,4-benzoquinone) and L32 (double deprotonated 2-(4-(isopropyl)anilino)-5hydroxy-1,4-benzoquinone) are two quinoid derivatives similar to L30. The former is symmetrical and the second has different donor sets at each site. In the case of L31 and L32, the corresponding dinuclear complexes $[Fe_2(L31)(CL4)_2](OTf)_2$ (**38**) and $[Fe_2(L32)(CL4)_2](OTf)_2$ (**39**) were prepared in order to compare a symmetric complex with the asymmetric one.[73] Complex **38** behaves in a similar way to **37** and its analogues (see above), exhibiting an incomplete SCO, structured in two steps (one more gradual than the other) with higher $T_{1/2}$. At low temperature, evidence of ferromagnetic coupling within [HS–HS] species is also observed here. The authors propose that the low temperature regime contains [LS–LS], [LS–HS] and [HS–HS], following two subsequent and incomplete SCO processes from [HS–HS] to [LS–HS], and then from the latter to [LS–LS]. The asymmetric analogue (**39**) exhibits a much cleaner SCO from a mixed spin system (1:1 HS and LS) to a [HS–HS] with a wide hysteresis. The low temperature regime does not indicate any kind of exchange coupling, suggesting that the system is composed exclusively of [LS–HS] species.

2.2 Trinuclear Complexes

Most of the trinuclear Fe(II) complexes exhibiting spin transition reported recently are linear species of three metal ions linked pairwise by triple bridges made of 1,2,4-triazoles. The early examples consist of three Fe(II) in the HS state, of which the central one, with a FeN_6 coordination environment, undergoes a spin transition to the LS state upon cooling.[74-76] These molecules always respond to the general formula $[Fe_3(trz)_6(L)_6](A)_6$, where trz is a triazole ligand, L are neutral monodentate ligands (usually solvent molecules) and A^- is a counterion. Very

recently, an interesting variation of this pattern was reported, using a 1,2,4-triazole bridging ligand bearing a negatively charged substituent; 4-(1,2,4-triazol-4-yl)ethanesulfonate (L33).[77] The reaction of an organic salt of L33 with $Fe(ClO_4)_2$ in water led to $[Fe_3(L33)_6(H_2O)_6]$ (**40**) the first neutral cluster of its kind. This compound crystallizes with several molecules of water. It features three HS Fe(II) ions at room temperature and experiences SCO of the central one. Complex **40** is partially desolvated above room temperature. The new phase is [HS–LS–HS] and reaches the [HS–HS–HS] state above 350 K. This SCO features a wide hysteresis in a remarkable case of high temperature cooperativity for a discrete compound ($T_{1/2}\uparrow$ = 357 K and $T_{1/2}\downarrow$ = 343 K). Interestingly, the system can be further desolvated by heating above 370 K. The resulting phase remains [HS–HS–HS] at all temperatures. The three phases and their transitions following desolvation were characterized by powder X-ray diffraction. A remarkable extension of this interesting avenue was made with the use of the dianionic triazole 4-(1,2,4-triazol-4-yl)ethanedisulfonate (L34) as bridging ligand. The resulting trinuclear complex with Fe(II) is then anionic, necessitating cations to achieve electroneutrality with formula $(Me_2NH_2)_6[Fe_3(L34)_6(H_2O)_6]$ (**41**).[78] At room temperature and below, compound **41** is found in the familiar [HS–LS–HS] state. Above 400 K, it converts into another phase that exhibits the [HS–HS–HS] state. This phase shows remarkable properties; it features a reversible [HS–HS–HS] to [HS–LS–HS] SCO associated to a wide hysteresis ($T_{1/2}\downarrow$ = 310 K, when cooling down at almost static scan rate). The [HS–HS–HS] state is easily trapped thermally at low temperature, and this metastable stable state only relaxes to the stable [HS–LS–HS] state when the temperature reaches T_{TIESST} = 250 K, the highest observed to date.

A triangular $[Fe(II)_3]$ cluster has been recently reported. It is made with the compartmental ligand L35 (3,5-bis-(6-(pyridine-2-yl)-pyridine-2-yl)-pyrazole), which has been originally designed to bind two octahedral metal ions occupying three *mer* coordination positions of each, leading to tetranuclear grid assemblies of composition $[M_4(L35)_4]^{n+}$. Some of them have shown multistep SCO processes, following the sequential transition of some of their individual metal centers.[79] By reducing the amount of $Fe(BF_4)_2$ in its reaction with L35, a defect grid $[Fe_3(L35')_2(L35)_2](BF_4)_2$ (L35', deprotonated L35; **42**) was obtained.[80] This compound crystallizes from MeCN with two solvent lattice molecules and exhibits the [LS-HS-LS] state between 2 and 380 K in a closed container. SCXRD data show that the central Fe(II) center is the one in the HS state. If complex **42** is deprived of the solvent lattice molecules by heating it in an open container, the system shows a [LS-HS-LS] to [LS-HS-HS] SCO with hysteresis ($T_{1/2}\uparrow$=355 K and $T_{1/2}\downarrow$ = 329 K). It was found that this hysteresis experienced consecutive widening with repeated cycling. This was shown to be caused by the gradual reduction of crystal sizes. Desolvated **42** showed also to be sensitive to the vapors of small molecules, in all cases drastically reducing or quenching the SCO altogether.

2.3 Coordination Polymers

SCO coordination polymers are built from polydentate ligands able to act as bridges between the active metal centers, thus creating a true infinite coordination structure in addition to furnishing the appropriate ligand field strength to observe this phenomenon. Only few multidentate ligands can match these two requirements. In most cases, combinations of ligand types are necessary, including ancillary terminal ligands, to achieve all these conditions. The coordination modes, local geometry and ligand skeleton will modulate the network dimensionality.

In this section, we have classified the different materials based on their bridging ligands, as a means to further understand their activity and effect upon the magnetic bistability. A very comprehensive and detailed review on SCO coordination polymers was published in 2013 by Muñoz, Real *et al*.[15] Because of this, we will focus on the most recent 2013-2017 literature to cover the significant advances in the field and some future trends.

It is easy to derive that coordination polymers are more prone to exhibit high cooperativity SCO, given the long-range connectivity between active centers mediated by the bridging ligands. In general, this should yield abrupt transitions, and wide hysteresis, and these was the initial driving force for their study. This is however not always the case, and many polymeric structures also exhibit non-cooperative transitions, including incomplete or multi-step transitions with intermediate phases. As discussed in the introduction, the latter is also an attractive possibility with unique technological applications.

The polymeric nature of these materials also gives them an especial stability in the solid state, allowing the reversible incorporation of guest molecules in their structure. Post-synthetic exchanges of solvent, and organic molecules, in addition to chemical reactions within their robust architecture offer unparalleled possibilities in the field, since molecular SCO materials are prone to irreversible changes upon desolvation or solid-state solvent exchange reactions. A comprehensive review on guest chemistry of SCO coordination polymers was recently published by Cirera.[81]

2.3.1 Polymers with 1,2,4-triazole ligands

1,2,4-triazole (L36) and its derivatives have been exploited for decades as a source of high temperature, wide thermal hysteresis SCO materials.[82-84] Easy preparation from readily available raw materials in combination with their robust and abrupt thermal transitions at/above room temperature made them unique candidates for memory devices and sensors. The materials of this family are formed by triply-bridged Fe 1D chains, where all Fe centers are structurally identical, possessing an N_6 coordination (Figure 6).[16, 85-87] The bistability and magnetic features of these materials, despite their stiff architecture, may be tuned by modification on the triazole functional group on the N4 position, by the anions compensating the overall cationic charge (the ligands are typically neutral), and by the solvent content. Variations of these main elements have been exploited for the last decades, and little surprises are expected.

Most efforts are currently being directed to their exploitation at the nanoscale.[85, 88-89] Remarkably, these materials retain the memory effect down to very small sizes (< 5 nm),[90-91] including core/shell architectures.[92]

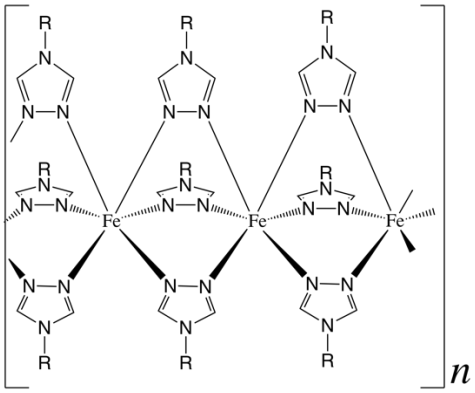

Figure 6. Scheme of the triazole-bridged Fe^{II} 1D chains. Structural base for most triazole-based SCO coordination polymers.

Another interesting research line is the use of these robust materials as components for multifunctional composites in the search for synergy. The most relevant results were found in combination with organic conductors,[93] and elastic polymers, [94]where the spin transition triggers (tunes) the polymer properties. The latter case is particularly appealing since it opens a new field of application for SCO compounds as components for actuators.[95]

Optical activity has also been introduced in this family, by using a chiral anion to neutralize the charge of the cationic chains.[96] Synergy between both properties generates switchable chiro-optical features. Additionally, this strategy also promotes molecular recognition. For instance, $[Fe(L37)_3](R\text{-}CSA)$ (**43**; L37 = 4-amino-1,2,4-triazole; R-CSA = R-camphorsulfonate) is sensitive to the inclusion of chiral guests.[97] Although changes in transition temperatures are small (< 2 K), it was concluded that this material can distinguish between R- or S-2-butanol, as detected by magnetic or spectroscopic techniques.

Some interesting attempts to improve the processability of these materials have been reported recently. For example, films of $[Fe(L38)_3](DBS)_2$ (**44**; DBS = 4-dodecylbenzenesulfonate; L38 = 4-dodecaoctyl-1,2,4-triazole), possessing substituted with long alkyl chains, can be spin-coated from an homogeneous suspension of the material in common solvents. This long alkyl chain ligands decrease cooperativity, but maintain room temperature bistability.[7] This technique also allowed for the processing of thermochromic fibers.[98]

Substitution at the N4 position with other groups, such as alkylcarboxylates, was also studied. The use of ethyl-1,2,4-triazol-4-yl-propionate (L39) yielded the first case of a two-step spin transition in these compounds in the corresponding BF_4^- salt $[Fe(L39)_3](BF_4)_2$ (**45**).[99] With the related ligand ethyl-4H-1,2,4-triazol-4-yl-acetate (L40), a complete $[Fe(L40)_3]X_2{\cdot}xS$ (**46**; X= various anions; S=solvent) series was obtained, tuning the memory effect at, below and above room temperature with different anions and solvent content. A widest thermal hysteresis of 60 K was found for the NO_3^-, solvent free derivative.[100]

The robust and reliable spin transition of these 1D derivatives has also been exploited for the preparation of a variety of sensors. For example, a pressure sensor was developed with $[Fe(L41)_3]I_2{\cdot}H_2O$ (**47**; L41 = 4-(2'-hydroxyethyl)-1,2,4-triazole).[101]

2.3.2 Polymers with cyanide ligands

Cyanometallates (Figure 7) have been very useful building blocks for the development of molecule-based materials due to their double function. On the one hand, they act as multidentate ligands for transition metal cations via the N-end of the cyanide moieties; at the same time, they act as functional units, due to their electro-active metal-cores. The combination of cyanometallates with a second metal cation yields the large family of Prussian blue (PB) derivatives;[102] an extended family of three-dimensional coordination polymers. The extreme ligand field difference between both ends of the cyanide ligand, *i.e.* very strong field at the C-end and weak by the N-end, has not promoted the appearance of SCO in pure PB analogs, although they show often SCO-related phenomena involving charge transfer processes.[103]

The structure of these materials can be tuned by incorporation of additional ligands, which break the 3D network and, more importantly, modify the crystal field around the second metal cation. This strategy was very successful for the development of spin crossover materials. The first examples appeared by combining square planar tetracyanometallates, $[M(CN)_4]^{n-}$, with bridging N-heterocycles, such as pyrazine (L42). In these clathrates, Fe^{II} octahedral centers are coordinated by four weak ligands (cyanometalates) on the equatorial positions; and by two relatively strong field ligands (*eg.* pyrazine) at the axial positions, connecting two adjacent layers. This combination forms a 3D network (Figure 8) exhibiting a cooperative spin transition,[104-106] even as nanoparticles (<2 nm).[107-108] Very fast spin transitions (≈ 20 ps) have been found in nanocrystals of the classical compound [Fe(L42)Pt(CN)$_4$] (**48**), with dimensions below 25 nm.[109] This confirms that SCO transitions may be fast enough for applications in information storage.

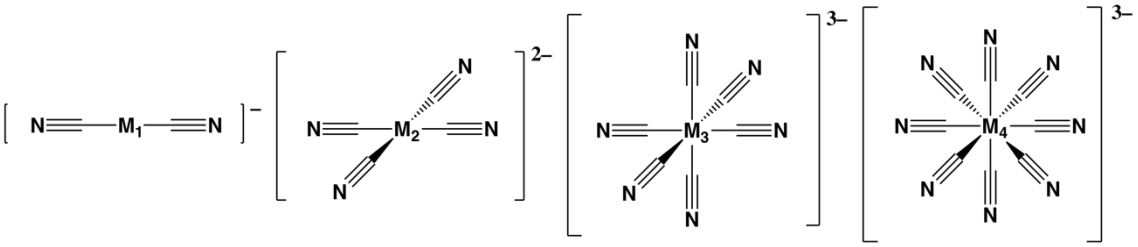

Figure 7. Cyanometallates bridging ligands for the construction of spin crossover polymers. M1 = Ag, Au; M2 = Ni, Pd, Pt; M3 = Fe, Co; M4 = Nb

One of the most interesting prospects for these materials is the possibility to switch between spin states at high temperatures through electromagnetic irradiation. Through a mechanism different to the LIESST phenomena, these materials have shown light-controlled bistability within the thermal hysteresis cycle.[110-112]

One of the most recent developments was the observation of a four-step spin crossover in the material $[Fe(L43)(Au(CN)_2)_2]\cdot x$EtOH (**49**; L43 = 3,6-bis(4-pyridyl)-1,2-diazine).[113] Remarkably, this compound can be obtained from its components, but also from post-functionalization of a preformed derivative, by a solid state reaction.[114] It is also remarkable that all Fe ions are equivalent in the full HS or LS states, but the compound changes lattice and periodicity to stabilize phases with inequivalent Fe(II) sites of variable LS/HS ratios. Theoretically, multistep switchable cooperative solids could open the way for three- or several-bit electronics,[115] and this family of materials is particularly prone to this

phenomenon. A three-step transition was also found in the related clathrate $[Fe(L44)Pt(CN)_4]$ (**50**; L44 = S,S'-bis-(4-pyridyl)methylenedithiolate.[116]
The record temperature for this type of materials was obtained for the compound $[Fe(L42)(Au(CN)_2)_2]$ (**51**), an interpenetrated solvent free 3D network.[117] This dense structure exhibits an 18 K wide hysteresis loop above 340 K. The isostructural silver analog $[Fe(L42)(Ag(CN)_2)_2]$ (**52**) was reported as diamagnetic at room temperature,[118] and only very recently, its high temperature behavior has been studied. As the Au compound, a hysteresis loop appears at very similar temperatures.[119] The major difference is that the Ag analog needs to be first desolvated to show bistability.

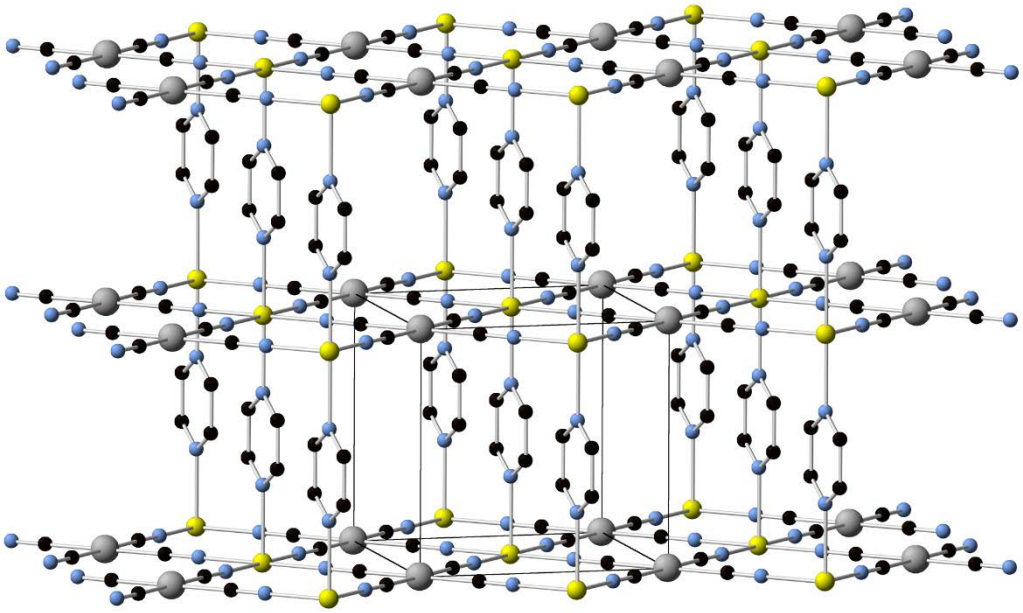

Figure 8. 3D network in the $[Fe(L42)Pt(CN)_4]$ (**48**) crystal structure (Fe, yellow; Pt, grey; C, black; N, light blue. H-atoms omitted for clarity).[109]

When the bridging bis-monodentate ligand is long enough, interpenetrated 3D structures are typically observed. An interpenetrated 3D network is obtained from the combination of $[Fe(L45)_2(Au(CN)_2)_2]\cdot(GM)$ (**53**; L45 = 2,5-bis(pyrid-4-yl)pyridine; GM = guest molecule). This ligand has an uncoordinated nitrogen atom to act as H acceptor. The hysteretic transition of this material is extremely sensitive to the guest molecules, with tunable transition temperatures over a range of 130 K, being lower for non-polar guests ($T_{1/2}$ > 120 K for *S* = cyclohexane) and increasing with polar guests ($T_{1/2}$ > 250 K for *S* = isopropanol).[120]
Flexible ligands, such as N,N'-bis(4-pyridylmethyl)piperazine (L46), yield interpenetrated 3D polymers with linear $[M(CN)_2]^-$ dicyanometallates, $[Fe(L46)(M(CN)_2)_2]$ (M = Au, **54**; Ag, **55**), but not with the square planar $[Ni(CN)_4]^{2-}$. The interpenetrated networks show spin transitions, more abrupt for the Ag derivative, while the Ni analog is a HS compound.[121]
As mentioned above, the robust 3D structure of these clathrates, allows for reversible incorporation of guest molecules into their porous structure. Guest effects have been also recently reviewed. [122] An interesting approach, regarding the effect of guest molecules on the magnetic features, is the use of functional molecules, which can be further modified *in situ* to tune the transition. This was achieved by incorporation of maleic anhydride into the classic $[Fe(L42)Pt(CN)_4]$

(**48**) clathrates. Humid atmosphere easily hydrolyzes the anhydride yielding maleic acid, while heating induces the reverse transformation. This allows a perfect control upon the spin transition from 275 K for the empty material, down to 200/170 K (2-step) for the anhydride guest, and to 150 K (incomplete) for the acid guest.[123]

Guest effects were also studied for the expanded framework $[Fe(L23)Pt(CN)_4]$ (**56**). This material can host relatively large molecules, such as stilbene. The guest molecule also affects significantly the magnetic properties, what has been ascribed to the flexibility of the bridging ligand.[124] The expanded 3D network $[Fe(L47)(Au(CN)_2)_2]$ (**57**; L47 = 1,4-bis(4-pyridyl)benzene) is especially sensitive to aromatic guests, with a record 73 K wide thermal hysteresis when naphthalene is incorporated into this porous structure. Comparatively, no hysteresis is observed when using simple benzene molecules instead.[125]

Another guest-sensitive 3D polymer is $[Fe(L20)(Au(CN)_2)_2]$ (**58**). The cubic holes in this structure can be occupied by a variety of organic molecules, from benzene to *p*-xylene. This small modification in the size of the guest promotes a change in the spin transition of over 30 K. The transition temperature decreases down 50 K when the aromatic guest is substituted by chloroform, another fine example of the subtlety of the spin transition phenomena.[126] The related $[Fe(L20)Ni(CN)_4]$ (**59**) is also sensitive to ethanol, or acetone vapors, changing from two-step to one-step spin transitions.[127]

Tris-monodentate ligands have also yielded 3D polymers with dicyanometallates. In this case, pillared structures are formed with hexagonal planes linked by the dicyanometallates, yielding porous 3D polymers.[128] $[Fe(L48)_{2/3}(M^I(CN)_2)_2]$ (**60**; L48 = 2,4,6-tris(4-pyridyl)-1,3,5-triazine; M^I = Ag, Au) for instance, can reversibly incorporate aromatic rings. It is remarkable that five membered rings of almost identical sizes (furan, pyrrole and thiophene) can be distinguished by these clathrates, resulting in modifications of up to 60 K in $T_{1/2}$.[129] This is a remarkable example of the subtlety of SCO phenomena.

Enhanced porosity has been achieved with extremely long bis-monodentate ligands, such as 1,4-bis(4-pyridylethynyl)benzene (L49), which is part of the framework $[Fe(L49)M(CN)_4]$ (M = Pt, **61**; Pd, **62**; Ni, **63**). The host-guest chemistry of these materials has not been exploited yet, but promising results are envisioned in light of the effect observed preliminary for solvation/desolvation upon the SCO features.[130]

Analogous clathrates were also obtained with the planar $[Pd^{II}(SCN)_4]^{2-}$ anions. For example, $[Fe(L42)Pd(SCN)_4]$ (**64**) is HS at all temperatures at ambient pressure, due to the weaker ligand field with respect to $[Pd^{II}(CN)_4]^{2-}$. Under pressure, spin transition behavior appears, resulting in an almost complete transition above 0.9 GPa.[131]

The use of substituted pyrazines, such as 2-fluoropyrazine (L50), also yields the classic pillared 3D structure.[132] An interpenetrated 3D network was obtained as $[Fe(L50)(Au(CN)_2)_2]$ (**65**), showing a robust 40 K wide hysteresis cycle, in the 220–270 K range. However, depending on preparation conditions, L50 may also act as terminal ligand. Terminal ligands (Figure 4), such as pyridine (CL6),[133-134] occupy the axial positions, isolating the cyanide-bridged tetragonal 2D network. These layered structures have also shown interesting spin crossover phenomena.

The L50 analogs, chloro- and 2-methyl-pyrazine (CL7, CL8), only yield 2D networks, acting as pyridine-like terminal ligands, as in $[Fe(CL7)_2M(CN)_4]$ (**66**, M = Ni, Pd, Pt; Figure 9).[135] All these materials show spin transition with significant thermal hysteresis cycles, up to 30 K wide. The one with 3-aminopyridine (CL9) is an interesting case where the change from Ni to Pd or Pt severely affects the hysteresis of the spin transition, in width (from 27 to 37 K) and position (from 150 up to 190 K).[136] Hydrogen bonding promoted by the amine group was identified as responsible for the enhanced cooperativity in these compounds. 4-X-Pyridine (CL10), where X is Cl, Br or I, yield 2D isostructural coordination polymers with $[Au(CN)_2]$, *e.g.* $[Fe(CL10)_2((Au(CN)_2)_2]$ (**67**; X=Cl), exhibiting a significant effect of the halide on the spin transition cooperativity, from abrupt to gradual.[137] A lower transition temperature and no hysteresis were found, for example, on the compound $[Fe(CL11)_2(Au(CN)_2)_2]$ (**68**; CL11 = 4-(3-pentyl)pyridine), with a large aliphatic substituent on the pyridine-like ligand.[138]

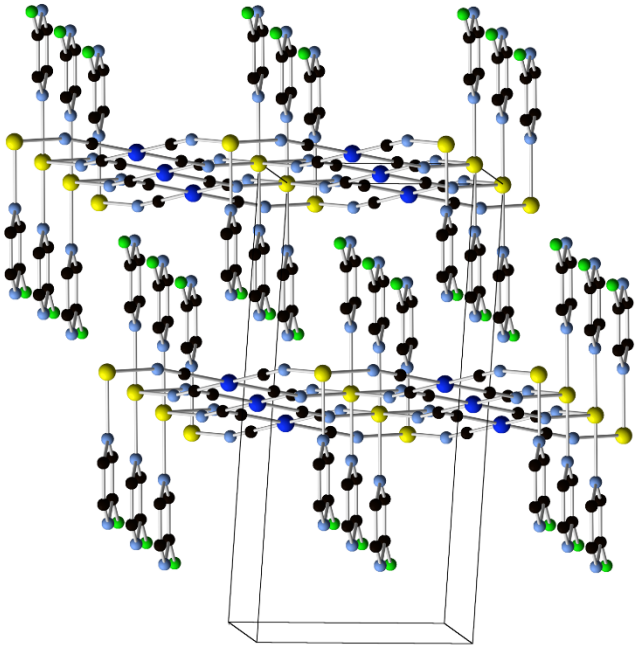

Figure 9. 2D network in the $[Fe(CL7)_2Ni(CN)_4]$ (**66**) crystal structure. (Fe, yellow; Ni, deep blue; C, black; N, light blue; Cl, green. H-atoms omitted for clarity).[135]

Some 1,2,4-triazole ligands may also act as terminal ligands in combination with cyanometallates to yield 2D networks. This is the case of L3 in the 2D material $[Fe(L3)_2Pt(CN)_4]$ (**69**). The L3 ligands are interdigitated between layers, creating two inequivalent Fe(II) sites. There is a first order spin transition from a fully HS state to an intermediate LS-HS state, while the ground LS state can only be accessed via reverse-LIESST effect. The strong metastability of the intermediate state was correlated to the antiferroelastic interactions between layers.[139]
A two dimensional network was also obtained with 5-methyl-2-(thienyl)vinyl-1,2,4-triazole (CL12).[140] This ligand occupies the axial positions of the Fe(II) centers in $[Fe(CL12)_2Pd(CN)_4]\cdot nH_2O$ (**70**). This material is particularly interesting since in the hydrated form is a HS compound, but an abrupt transition with a ≈20 K wide hysteresis appears upon dehydration. Spin transition can also be induced under pressure but in this case, the material goes through a two-step process.

This illustrates the importance of the crystallographic transitions associated to SCO when it comes to promote cooperative phenomena.
If bis-dentate chelating ligands (instead of bismonodentate ligands) are combined with $[M(CN)_4]^{2-}$ moieties, the formation of a 3D or 2D structure is precluded, and 1D polymers are obtained. This is the case, for example, with 2-picolylamine (CL13) or 2-(1*H*-pyrazol-3-yl)-pyridine (CL14). The corresponding zig zag chains $[Fe(CL13)_2M(CN)_4]$ (**71**, Figure 10) and $[Fe(CL14)_2M(CN)_4]$ (**72**; M = Pd, Pt) exhibit abrupt spin transitions between 100 K and 300 K depending on solvent and counter anions.[141] Only very narrow hysteresis were found in all these materials.

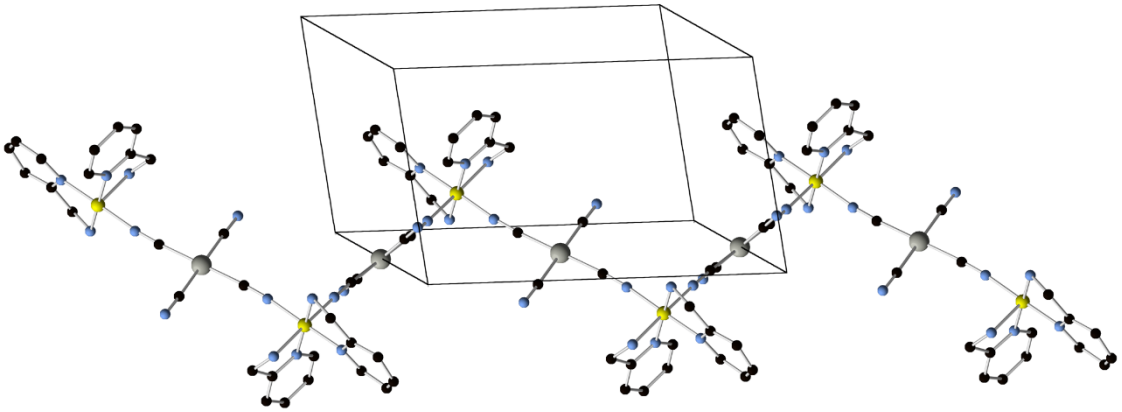

Figure 10. 1D network in the $[Fe(CL13)_2Pd(CN)_4]$ (**71**) crystal structure. (Fe, yellow; Pd, grey; C, black; N, light blue; Cl, green. H-atoms omitted for clarity).[141]

1D polymers are obtained with 4-amino-3,5-bis(pyridine-2-yl)-1,2,4-triazole (CL15) of formula $[Fe(CL15)_2M(CN)_4]$ (**73**; M = Pt, Ni). In this structure, the two CL15 ligands occupy the equatorial positions, and the chain grows through the $M(CN)_4$ bridging axial positions in *trans*. These chains are LS at room temperature while the HS is populated above 300 K, although decomposition occurs before the transition is complete.[142-143]
Most examples described this far were obtained with linear dicyanometallates or square planar tetracyanometalates. Fewer examples have been reported with cyanometallates with higher coordination numbers. However, a remarkable example has been obtained with an octacyanometallate and the ancillary ligand 4-pyridinealdoxime (CL16); $[Fe_2(CL16)_8Nb(CN)_8]$ (**74**).[144] The spin transition is gradual, between 100 and 200 K. The unprecedented phenomenon occurs at low *T*, where the compound shows LIESST effect. Population of the HS state *via* irradiation triggers ferromagnetic exchange between both types of metal. As a result of this, the material becomes magnetizable and thus a molecular base magnet exhibiting a hysteresis. This represented the first reported LIESST-promoted magnet. Following this work, analogous phenomena were also observed using the simple pyrazole ligand (CL17), in $[Fe_2(CL17)_8Nb(CN)_8]\cdot 4H_2O$ (**75**),[145] although in this case the spin-crossover is pressure-induced. Another ligand that promotes SCO phenomena in octacyanide-based coordination polymers is (2-pyridyl)methanol (CL18), which leads to the product $[Fe_2(CL18)_8W(CN)_8]\cdot nH_2O$ (**76**) with a high dependence on hydration. In this case, only two positions on the Fe centers are occupied by CN ligands.[146]

2.3.3 Other ligands

There are few bridging ligands able to form binary (ML_n) coordination networks when combined with metal centers, providing ligand fields of the appropriate strength to bring bistability with a simple ML_6 coordination mode. The 1,2,4-triazole ligand is a major example, as described in section 2.3.1.

One interesting 1D chain is obtained with the rigid ligand 1,4-bis(tetrazol-1-ylmethyl)benzene (L51), which forms triple bridges between octahedral Fe(II) centers. The shape of this ligand creates a porous structure, $[Fe(L51)_3](ClO_4)_2$ (**77**), that recognizes CO_2 molecules.[147] The inclusion of these molecules from the gas phase induces a minor change (but measurable) in $T_{1/2}$. When this polymer is diluted in the solid state with the structurally analogous bis-triazole (L52), as a way to tune the spin transition, the weak ligand field of L51 brings down the $T_{1/2}$ from 200 K for the pure compound of tetrazole to 60 K for the solid solution (ratio 2/1). The all triazole compound $[Fe(L52)_3](ClO_4)_2$ (**78**) is HS.[148]

Ligand 1,3-di(tetrazol-1-yl)propane (L53), analogous to L51 with substitution of the benzene ring by a flexible alkyl chain, also forms 1D chains with formulae $[Fe(L53)_3]X_2$ (**79**; X=ClO_4^- or BF_4^-) with abrupt spin transitions and no hysteresis. Efficient LIESST effect was observed.[149] Several analogous 1,ω-di(azolyl)alkane-type ligands (L54) yield cationic 2D networks of formula $[Fe(L54)_3]^{2+}$ (**80**), typically with incomplete or gradual spin transitions, due to the flexibility/elasticity of the alkane chain.[150] The latter remains crystallographically disordered in the HS or the LS state, even under pressure or after light-induced transitions at very low temperature.

6,6'-Bis(1*H*-tetrazol-5-yl)-2-2'-bipyridine (L55) is a multidentate ligand that upon complete deprotonation yields a 2D neutral network [Fe(L55)] (**81**),[151] with the axial positions occupied by tetrazole units from adjacent complexes. This tetragonal network shows an abrupt spin transition, and it also exhibits complete LIESST at 10 K, revealing antiferromagnetic interactions between Fe(II) centers. Tetrazole-2-yl rings have been also combined with axially coordinated nitriles yielding also 2D networks, with gradual SCO, and effective LIESST effect.[152]

A two-dimensional tetragonal grid is obtained with 3-(5-bromo-2-pyridyl)-5-(4-pyridil)-1,2,4-triazole (L56), of composition $[Fe(L56)_2]$ (**82**), showing a 2-step spin transition. The flexibility of this network makes it sensitive to the presence of guest molecules, or to applied pressure, showing easy tuning of the SCO features.[153]

Another type of Fe/ligand polymer is obtained with trans-4,4'-azo-1,2,4-triazole (L57), $[Fe(L57)_3]X_2$ (**83**, X=ClO_4^- or BF_4^-), with spin transition close to room temperature.[154] These interpenetrated 3D networks are sensitive to humidity, which makes the transition more gradual and lowers the $T_{1/2}$ values. The resulting crystal structure, however, is identical to that of the dehydrated form.

3,5-substituted triazole ligands functionalized with pyridine groups, such as 3-(2-pyridyl)-5-(3-pyridyl)-1,2,4-triazole (L58), 2-(5-(4-(1H-imidazol-1yl)phenyl)-4H-1,2,4-triazol-3-yl)pyridine (L59), or 2-(5-(4-(pyridine-3-yl)phenyl)-4*H*-1,2,4-triazol-3-yl)-pyridine (L60), yield a series of solvent-less robust 2D Fe networks upon ligand deprotonation; $[Fe(L58)_2]$ (**84**), $[Fe(L59)_2]$ (**85**) and $[Fe(L60)_2]$ (**86**). These ligands possess a monodentate pyridyl or imidazolyl site and the triazol-pyridyl

chelating site, and their anionic nature avoids the need for counter anions. These coordination networks exhibit very high spin transition temperatures, specifically, **83** features the highest one reported (≥ 500 K).[155-156] This can be observed only thanks to their extremely high thermal stability. The spin transitions are gradual and most times incomplete.

Many other examples of SCO coordination networks are based on the combination of two different ligand types, one bridging and one capping. This reduces dimensionality, but increases the structural and chemical versatility. One of the most successful strategies is based on the combination of bispyridine-like ligands with NCS^- (or $NCSe^-$) anions, as capping ligands. For example, 1,2-bis(pyridine-4-ylmethylene)hydrazine (L61) creates porous materials of formula $[Fe(L61)_2(NCX)_2]$ (**87**), where the spin transition is highly dependent on guest molecules.[157] These materials tend to exhibit interpenetration, with the grid-like planes in two orthogonal directions. The same is observed for 1,4-bis(pyridin-4-yl)benzene (L47) in $[Fe(L47)_2(NCX)_2]$ (**88**) compounds. Substitution with the isoelectronic $NCBH_3^-$ anion slightly modifies the packing of the 2D layers, and increases the spin transition temperatures of the corresponding $[Fe(L47)_2(NCBH_3)_2]$ (**89**) polymers by 100 K.[158] Surprisingly, the analogous structure with L20, obtained with water groups substituting the NCX^- anions, $[Fe(L20)_2(H_2O)_2](ClO_4)_2$ (**90**), has been reported to exhibit a spin transition, being one of few examples where an Fe^{II} coordination material with weak ligand field water molecules shows SCO phenomena.[159]

Particularly interesting is the series of materials obtained from trans-(4,4'-vinylenedipyridine (L22), which participates of 2D interpenetrating networks[160] of formula $[Fe(L22)_2(SCN)_2]\cdot GM$ (**91**), where GM may be a variety of guest molecules, yielding inclusion derivatives. A detailed study on the effect of the guest molecule on the SCO properties indicate that the transition temperature is almost invariable, but the different size and nature of the ligands have strong influence in the cooperativity, promoting the appearance of small hysteresis.[161] In a related work, poly-4-vinylpyridine and its block copolymers have been used as nucleation matrix to template nanoparticle synthesis of coordination polymers, resulting in increased stability against degradation and excellent size control.[162-163]

Tris-monodentate ligands, such as 1,3,5-tris(4-pyridyl)benzene (L62) create a 3D structure (boracite-like) of formula $[(Fe(NCS)_2)_3(L62)_4]$ (**92**), with octahedral $Fe(N_4)(SCN)_2$ building blocks. This porous network shows an incomplete transition around 150 K, with little dependence on the nature of the guest molecules.[164] The tris-chelating ligand 1,4,5,8,9,19-hexazatriphenylene (L63) forms a 1D coordination polymer. Only two of the three chelating positions are binding to Fe(II) centers, creating a homochiral structure with formula $[Fe(L63)(NCS)_2]$ (**93**) that exhibits a two-step spin transition.[165]

A zig-zag chain, $[Fe(CL19)(L64)](BPh_4)_2$ (**94**), is obtained with 1,2-bis(pyridine-2-yl-methyl)thio]ethane (CL19) and the linker adiponitrile (L64).[166] Again, solvent dependent behavior was found, as seen very often with 1D systems. In this case, the counter anion is also important to favor the polymeric structure, since bulky inorganic anions such as SbF_6^- induce crystallization of a LS discrete dimer.

The combination of a salen-type (CL3) Fe^{II} complex and the bridging ligand 4,4'-dipyridylethyne (L21) gives 1D polymers, [Fe(CL3)(L21)] (**95**), with solvent-dependent SCO behavior. When desolvated, these materials exhibit a three-step spin transition.[62] Analogous 1D polymers have been reported with 3,3'-azopyridine (L65); [Fe(CL3)(L65)] (**96**). In this case, the spin transition shows very slow kinetics, favoring trapping of the HS state via fast cooling.[167]

The ligand tetra(4-pyridyl)tetrathiafulvalene (L66) was especially designed to incorporate multiple properties into a Fe^{II} coordination network, including spin transition. With additional dicyanamide (L67) bridging ligands, a 3D coordination network was obtained, [Fe(L66)(L67)](ClO_4) (**97**) exhibiting spin transition ($T_{1/2}$ = 146 K), LIESST effect, redox activity, and enhanced conductivity upon oxidative doping.[168]

There are few exceptions to the Fe^{II} paradigm in SCO coordination polymers. Only a small number of Co^{II} coordination networks belong to the family exhibiting this property. The compound [CoX_2(L68)] (**98**; X = Cl, Br) is one of the few non-iron SCO examples. Ligand L62 was particularly designed for the formation of 1D linear chains, with two opposite and different coordination sites. The SCO is solvent dependent, and shows no thermal memory effect.[169]
Another SCO 1D chain was obtained with the equatorial (N_4) ligand N-N'-(bis(pyridine-2-yl)benzylidine)ethane-1,2-diamine (CL20) with bridging L67. These chains are very sensitive to the nature of the counterions: abrupt with hysteresis in the case of ClO_4^-,[170] gradual in the case of PF_6^-.[171]

Table 1. A list of all SCO complexes featured in this review, together with the main parameters of their magnetic behavior.

Complex	Guest/solvent	D	$T_{1/2}(\uparrow)$	$T_{1/2}(\downarrow)$		Ref
$[Fe_2(L1)_5(NCS)_4]$ (**1**)	-	0D	150	=	abr.	[27]
$[Fe_2(L2)_5(NCS)_4]$ (**2**)	-	0D	115	=	inc.,gr.	[28]
$[Fe_2(L3)_5(NCS)_4]$ (**3**)	MeOH·EtOH	0D	116	=	inc.gr.	[29]
	H_2O	0D	-	-	HS	
$[Fe_2(L4)_5(NCS)_4]$ (**4**)	MeOH·EtOH	0D	116	=	inc.gr.	[30]
	EtOH	0D	122	=	inc.gr.	
$[Fe_2(L5)_5(NCS)_4]$ (**5**)	H_2O	0D	150	=	gr.	[31]
$[Fe_2(NCSe)_2(L7)_2(py)_2]$ (**6**)	-	0D	109	=	abr.	[36]
$[Fe_2(L9)_2(MeCN)_4](BF_4)_4$ (**7**)	MeCN	0D	369	356	inc.,gr.	[39]
$[Fe_2(L9)_2(EtOH)_4](BF_4)_4$ (**8**)	-	0D	-	-	HS	
$[Fe_2(L9)_2(H_2O)_4](BF_4)_4$ (**9**)	-	0D	-	-	HS	
$[Fe_2(L10)](X)_4$ (**10**)	variable	0D	Variable or undefined			[41]
$[Fe_2(L11)](BF_4)_4$ (**11**)	H_2O	0D	217	195	abr.	[24]
$[Fe_2(L12)]^{4+}$ (**12**); R=Ph	H_2O	0D	265 210 87	= = =	3-st. gr.	[43]
R= tolyl	$MeCN/H_2O$	0D	109	=	inc.gr.	
R= ^{i}Bu	$MeCN/H_2O$	0D	-	-	HS	
$[Fe_2(L13)](BF_4)_4$ (**13**)	DMF	0D	280	=	inc.gr.	[44]
$[Fe_2(L14)]X_4$ (**14**); X=ClO_4^-	MeCN	0D	140*	=	inc.abr.	[45]
X= BF_4^-			-	-	HS	
X= $CF_3SO_3^-$			173*	147*	inc.abr.	
$[Fe_2(L15)_3](BF_4)_4$ (**15**)		0D	-	-	HS	[50]
$[Fe_2(L16)_3](BF_4)_4$ (**16**)		0D	>400	und.	gr.	[50]
$[Fe_2(L17)_3](BF_4)_4$ (**17**)		0D	-	-	LS	[51]
$[Fe_2(L18)_2](PF_6)_4$ (**18**)	$MeCN/H_2O$	0D	426	437	inc.gr.	[52]
$Cl@[Fe_2(L19)_3]Cl(PF_6)_2$ (**19**)	MeOH	0D	265	und.	inc.gr.	[54]
$Br@[Fe_2(L19)_3]Br(PF_6)_2$ (**20**)	MeOH	0D	305	und.	inc.gr.	[54]
$[Fe_2(NCS)_4(CL1)_2(L20)]$ (**21**)	MeOH	0D	105*	105*	inc.gr.	[60]
$[Fe_2(NCS)_4(CL2)_2(L20)]$ (**22**)		0D	191 218	= =	2-st. gr.	[61]
$[Fe_2(CL3)_2(L21)(ROH)_2]$ (**23**)		0D	-	-	HS	[62]
$[Fe_2(NCS)_4(CL2)_2(L22)]$ (**24**)	(polym. 1) –	0D	132 215	= =	2-st. gr.	[63]
	(polym. 2) -		-	-	HS	
	MeOH		159	=	abr.	
$[Fe_2(NCBH_3)_4(CL2)_2(L20)]$ (**25**)		0D	203 223	= =	2-st. abr.	[65]
$[Fe_2(NCBH_3)_4(CL2)_2(L21)]$ (**26**)		0D	290	=	gr.	[65]
$[Fe_2(NCBH_3)_4(CL2)_2(L23)]$ (**27**)		0D	241	=	gr.	[65]
$[Fe_2(L24)_2(NCS)_4]\cdot$(**28**)	$4CH_2Cl_2$	0D	180 80	= =	2-st. gr.	[66]
	CH_2Cl_2		200	=	gr.	
$[Fe_2(L25)(H_2O)_2(MeOH)_2](ClO_4)_2$ (**29**)	MeOH	0D	-	-	HS	[68]
$[Fe_2(L25)(H_2O)_2(MeCN)_2](BF_4)_2$ (**30**)	MeCN	0D	265	=	inc.gr.	[68]
$[Fe_2(L25)Cl_2](CF_3SO_3)_2$ (**31**)	benzylcyanide	0D	-	-	HS	[68]
$[Fe_2(L26)_2(NCS)_2]$ (**32**)	DMF/H_2O	0D	125	und.	inc.gr.	[69]
	-		184	189	abr.	
$[Fe_2(L27)_2(NCS)_2]$ (**33**)	DMF/H_2O	0D	210 130	= =	2-st. gr.	[69]

Complex	Guest/solvent	D	$T_{1/2}(\uparrow)$	$T_{1/2}(\downarrow)$		Ref
$[Fe_2(SCN)_4(L28)_2]$ (**34**)	H_2O	0D	-	-	HS	[70]
$[Fe_2(L29)_2(CL4)_2]$ (**35**)	-	0D	350*	=	gr.	[71]
$[Fe_2(L29)_2(CL5)_2]$ (**36**)	MeOH	0D	180	=	gr.	[71]
	-		196	=	gr.	
$[Fe_2(L30)(CL4)_2](TFPB)_2$ (**37**) F-sub	THF/hexane	0D	160	=	gr.	[72]
Cl-sub			124	=	gr.	
Br-sub			121	=	gr.	
H-sub			110	=	gr.	
$[Fe_2(L31)(CL4)_2](OTf)_2$ (**38**)	CH_2Cl_2	0D	195 235	= 230	2-st. inc.gr.	[73]
$[Fe_2(L32)(CL4)_2](OTf)_2$ (**39**)	CH_2Cl_2/MeCN	0D	285*	230*	inc.gr.	[73]
$[Fe_3(L33)_6(H_2O)_6]$ (**40**)	H_2O phase 1	0D	150	=	inc.gr.	[77]
	H_2O phase 2		357	343	inc.abr.	
	-		-	-	HS	
$(Me_2NH_2)_6[Fe_3(L34)_6(H_2O)_6]$ (**41**)	H_2O	0D	>400	310	inc.gr.	[78]
$[Fe_3(L35')_2(L35)_2](BF_4)_2$ (**42**)	MeCN	0D	-	-	LS/HS/LS	[74]
	-		355	329	inc.abr.	
$[Fe(L37)_3]$(R-CSA) (**43**) R-CSA=camphorsulfonate	-	1D	316	300	gr.	[97]
	2-BuOH(rac)		324	315	abr.	
	R-2-BuOH		325	316	abr.	
	S-2-BuOH		323	314	abr.	
$[Fe(L38)_3](DBS)_2$ (**44**) DBS=4-dodecylbenzenesulfonate	-	1D	318	306	gr.	[98]
$[Fe(L39)_3](BF_4)_2$ (**45**)	-	1D	188 235	172 230	abr. 2-st.	[99]
$[Fe(L40)_3](X)_2$ (**46**) X= ClO_4^-	-	1D	296	291	abr.	[100]
	CH_3OH		273	263		
X= NO_3^-	-		338	278		
	H_2O		353	333		
X= BF_4^-	-		106	92		
	H_2O		320	305		
X= $CF_3SO_3^-$	H_2O		325	322		
$[Fe(L41)_3]I_2$ (**47**)	H_2O	1D	292	275	abr.	[101]
$[Fe(L42)Pt(CN)_4]$ (**48**)	-	3D	309	285	abr.	[109]
	maleic anhydride		209 186	200 170	2-st. abr.	
	maleic acid		159	155	inc.	
$[Fe(L43)(Au(CN)_2)_2]$ (**49**)	EtOH	3D	203* 178* 145* 107*	200* 172* 125* 85*	4-st.	[113]
$[Fe(L44)Pt(CN)_4]$ (**50**)	EtOH	3D	154 148 134	138 127 115	3-st.	[116]
$[Fe(L42)(Au(CN)_2)_2]$ (**51**)	-	3D	367	349	abr.	[117]
$[Fe(L45)_2(Au(CN)_2)_2]$ (**53**)	-	3D	148	=	gr.	[120]
	DMF/EtOH/ cyclochexane		153 134	143 126	2-st. gr.	
	cyclochexane		129	123	inc.	
	BuOH		209 189	186 171	2-st.	
	i-BuOH		222	217	2-st.	

Complex	Guest/solvent	D	$T_{1/2}(\uparrow)$	$T_{1/2}(\downarrow)$		Ref
			211	205		
	EtOH		251 226	249 208	2-st.	
[Fe(L46)(Au(CN)$_2$)$_2$] (**54**)	-	3D	204 134	= =	2-st.	[121]
[Fe(L46)(Ag(CN)$_2$)$_2$] (**55**)	-	3D	232 216	= =	2-st.	[121]
[Fe(L23)Pt(CN)$_4$] (**56**)	L23 H_2O	3D	240 216 200	= 212 197	3-st.	[124]
	L23		210 181 164	= 178 160		
	1,2-dibenzylethane		160*	=	gr.	
	stilbene		163	=	abr.	
[Fe(L47)(Au(CN)$_2$)$_2$] (**57**)	DMF,EtOH,C_6H_{12}	3D	175	=	gr.	[125]
	C_6H_{12}		142	136	inc.	
	C_6H_6		221 155 144	207 155 139	3-st.	
	CS_2		190	167	abr.	
	naphthalene		214	141	abr. inc.	
	ferrocene		166	129	gr. inc.	
	anthracene		151	131	gr. inc.	
	-		156 119	156 110	2-st.	
[Fe(L20)(Au(CN)$_2$)$_2$] (**58**)	benzene	3D	233	222	abr.	[126]
	toluene		234	231		
	o-xylene		220 184 136	217 176 132	3-st.	
	m-xylene		234 208	232 206	2-st.	
	p-xylene		266 214 185	246 212 182	3-st.	
	chloroform		184	128	inc.	
[Fe(L20)Ni(CN)$_4$] (**59**)	H_2O	3D	-	-	HS	[127]
	EtOH		223 197	213 187	2-st.	
	acetone		145	125	abr.	
[Fe(L48)$_{2/3}$(M(CN)$_2$)$_2$] (**60**); M=Ag	CH_2Cl_2	3D	244	=	gr.	[129]
	furan		209	=		
	pyrrole		167	=		
	thiophene		152	=		
M=Au	CH_2Cl_2		222	=		
	furan		199	=		
	pyrrole		197	=		
	thiophene		137	=		
[Fe(L50)(Au(CN)$_2$)$_2$] (**65**)		3D	263	221	abr.	[132]
[Fe(CL7)$_2$M(CN)$_4$] (**66**); M=Ni		2D	198 182	190 173	2-st. abr.	[135]
M=Pd			215 150	205 145	2-st. gr.	

Complex	Guest/solvent	D	$T_{1/2}(\uparrow)$	$T_{1/2}(\downarrow)$		Ref
M=Pt			115	101	abr.	
$[Fe(CL10)_2(Au(CN)_2)_2]$ (**67**)		2D	222*	218*	abr.	[137]
$[Fe(CL11)_2(Au(CN)_2)_2]$ (**68**)	CL11	2D 2D	250 93	250 92	2-st.	[138]
	-		124	=	gr.	
$[Fe(L3)_2Pt(CN)_4]$ (**69**)	-	2D	154	152	inc.	[139]
$[Fe(CL12)_2Pd(CN)_4]\cdot nH_2O$ (**70**)	-	2D	204	184	abr.	[140]
$[Fe(CL13)_2M(CN)_4]$ (**71**); M=Pd	-	1D	272	270	gr.	[141]
M=Pt	-		274	272		
$[Fe(CL14)_2M(CN)_4]$ (**72**); M=Pd	-	1D	186	=	abr.	
M=Pt			184	=		
$[Fe(CL15)_2M(CN)_4]$ (**73**)	-	1D	350*	=	gr. inc.	[142-143]
$[Fe_2(CL16)_8Nb(CN)_8]$ (**74**)	-	3D	130	=	gr.	[144]
$[Fe_2(CL18)_8W(CN)_8]\cdot nH_2O$ (**76**)	H_2O	3D	200	=	gr.	[146]
$[Fe(L51)_3](ClO_4)_2$ (**77**)	-	1D	204	200	gr.	[147]
	CO_2		212	209		
$[Fe(L53)_3]X_2$ (**79**) X=ClO_4^-	-	1D	150	149	abr.	[149]
X=BF_4^-			161	158		
$[Fe(L54)_3](ClO_4)_2$ (**80**)	MeCN	1D	165 96	165 90	2-st.	[150]
[Fe(L55)] (**81**)		2D	226	218	abr.	[151]
$[Fe(L56)_2]$ (**82**)	-	2D	192 144	=	2-st.	[153]
	MeOH		176 128	173 127		
	EtOH		158 121	154 113		
$Fe(L57)_3]X_2$ (**83**) X=ClO_4^-	H_2O	3D	265	=	abr.	[154]
	-		285	=		
X=BF_4^-	H_2O		284	=		
	-		290	=		
$[Fe(L58)_2]$ (**84**)			501 329	=	2-st. gr.	[155-156]
$[Fe(L59)_2]$ (**85**)			419	=	gr.	[155-156]
$[Fe(L60)_2]$ (**86**)			416	=	gr.	[155-156]
$[Fe(L61)_2(NCX)_2]$ (**87**)	MeCN	2D	129 78	=	2-st.	[157]
	acetone		90*	-	inc.	
$[Fe(L47)_2(NCX)_2]$ (**88**); NCS^-	EtOH/H_2O	3D	-	-	HS	[158]
	EtOH	2D	-	-	HS	
$NCSe^-$	EtOH/H_2O	3D	82	=	inc.	
	CH_2Cl_2 EtOH/H_2O	3D	96	=		
$[Fe(L47)_2(NCBH_3)_2]$ (**89**)	EtOH/H_2O	2D	247	=	abr.	[158]
	EtOH/CL_2CH_2		189	=	abr.	
$[Fe(L20)_2(H_2O)_2](ClO_4)_2$ (**90**)	L20 H_2O	2D	200*	=	gr.	[159]
$[Fe(L22)_2(SCN)_2]\cdot S$ (**91**) S=various guests	PhCHO	2D	194 176	194 168	2-st. gr.	[160]
	MeCN,H_2O	223 204		=	2-st. gr.	
	DMSO,H_2O	195		=	2-st.	

Complex	Guest/solvent	D	$T_{1/2}(\uparrow)$	$T_{1/2}(\downarrow)$		Ref
		163			gr.	
	DMA,H_2O	187 145		=	2-st. gr.	
	L22,H_2O	221 204		= 201	2-st. gr.	
	PhCN		224 202	224 198	2-st. abr.	
	$PhNO_2$		226 197	226 191	2-st. gr.	
	-		-	-	HS	
$[(Fe(NCS)_2)_3(L62)_4]$ (**92**)	CH_2Cl_2 EtOH	3D	152	142	gr.	[164]
$[Fe(L63)(NCS)_2]$ (**93**)	MeOH	1D	≈300	=	inc.	[165]
	-		358 172	=	2-st. gr.	
$[Fe(CL19)(L64)](BPh_4)_2$ (**94**)	acetone	1D	-	-	HS	[166]
	-		212	=	gr.	
[Fe(CL3)(L21)] (**95**)	EtOH	1D	190 135	170 110	2-st. abr.	[62]
	DMF		305	=	gr.	
	toluene		125	=	gr.	
	(annealed)	?	320 210 140	=	3-st. gr.	
[Fe(CL3)(L65)] (**96**)		1D	105	90	inc.	[167]
$[Fe(L66)(L67)](ClO_4)$ (**97**)		2D	146	=	inc.	[168]

*estimated from graphic plot. $T_{1/2}(\uparrow)$ and $T_{1/2}(\downarrow)$ are the temperatures (in K) of the thermal spin crossover upon warming and cooling, respectively, defined as the temperature where 50% of the conversion occurs with respect to the total number of centers that experience the transition.

3. Conclusions

This revision shows that SCO research continues to attract great interest. One of the pillars of progress in this field is synthetic chemistry, which is the source of the objects of study of the phenomenon. These should enable to gather fundamental knowledge surrounding this property and are bound to constitute the physical systems that shall be used to implement potential applications. It becomes very clear in this manuscript that the production of novel SCO polynuclear complexes has remained a very prolific activity during the last few years.

The use of new ligands, and combination of new and old organic linkers is paramount in order to unveil new aspects on the SCO phenomenon as well as for the ambitious goal of combining the spin switching property with other molecular functions. As described, we have found the major research lines in this field to be built towards several major objectives. As expected and predicted in our introduction, multi-step transitions and high temperature transition keep moving the field of polynuclear complexes further. Still, recent literature has brought some additional and unique opportunities for these compounds. On one hand, the promising appearance of dynamic effects (slow relaxation from the HS excited state) in these systems opens the possible development of single-molecules bearing memory effect. In the past, memory effect was exclusively associated to bulk materials. Another fascinating possibility is the processing of these polynuclear molecules or coordination networks as nanostructures

(monolayers, or thin films). Combination of these two future developments is one of the challenges for molecular magnetism and coordination chemistry. Polynuclear entities with memory effect at the nano-scale, at technologically relevant temperatures, remains one of the holy grails in molecular magnetism. In our opinion, polynuclear SCO are the most promising systems to achieve such a target in the near future.

4. References

[1] P. Gütlich, A. B. Gaspar, Y. Garcia, *Beilstein J. Org. Chem.* **2013**, *9*, 342-391.
[2] A. Urtizberea, O. Roubeau, *Chem. Sci.* **2017**, *8*, 2290-2295.
[3] Y. Jiao, J. P. Zhu, Y. Guo, W. J. He, Z. J. Guo, *J. Mater. Chem. C* **2017**, *5*, 5214-5222.
[4] G. A. Craig, J. S. Costa, O. Roubeau, S. J. Teat, H. J. Shepherd, M. Lopes, G. Molnar, A. Bousseksou, G. Aromi, *Dalton Trans.* **2014**, *43*, 729-737.
[5] F. Guillaume, Y. A. Tobon, S. Bonhommeau, J. F. Letard, L. Moulet, E. Freysz, *Chem. Phys. Lett.* **2014**, *604*, 105-109.
[6] C. Faulmann, K. Jacob, S. Dorbes, S. Lampert, I. Malfant, M. L. Doublet, L. Valade, J. A. Real, *Inorg. Chem.* **2007**, *46*, 8548-8559.
[7] G. Bovo, I. Braunlich, W. R. Caseri, N. Stingelin, T. D. Anthopoulos, K. G. Sandeman, D. D. C. Bradley, P. N. Stavrinou, *J. Mater. Chem. C* **2016**, *4*, 6240-6248.
[8] A. Diaconu, S. L. Lupu, I. Rusu, I. M. Risca, L. Salmon, G. Molnar, A. Bousseksou, P. Demont, A. Rotaru, *J. Phys. Chem. Lett.* **2017**, *8*, 3147-3151.
[9] A. Iazzolino, G. Galle, J. Degert, J. F. Letard, E. Freysz, *Chem. Phys. Lett.* **2015**, *641*, 14-19.
[10] P. L. Holland, *Acc. Chem. Res.* **2015**, *48*, 1696-1702.
[11] S. Samanta, S. Demesko, S. Dechert, F. Meyer, *Angew. Chem. Int. Ed.* **2015**, *54*, 583-587.
[12] M. A. Halcrow, *Chem. Soc. Rev.* **2011**, *40*, 4119-4142.
[13] M. A. Halcrow, *Chem. Lett.* **2014**, *43*, 1178-1188.
[14] J. Olguín, S. Brooker, in *Spin-Crossover Materials*, John Wiley & Sons Ltd, **2013**, pp. 77-120.
[15] M. Carmen Muñoz, J. Antonio Real, in *Spin-Crossover Materials*, John Wiley & Sons Ltd, **2013**, pp. 121-146.
[16] G. Aromi, L. A. Barrios, O. Roubeau, P. Gamez, *Coord. Chem. Rev.* **2011**, *255*, 485-546.
[17] J. Olguin, S. Brooker, *Coord. Chem. Rev.* **2011**, *255*, 203-240.
[18] O. Roubeau, *Chem., Eur. J.* **2012**, *18*, 15230-15244.
[19] M. A. Halcrow, *Coord. Chem. Rev.* **2009**, *253*, 2493-2514.
[20] G. A. Craig, O. Roubeau, G. Aromi, *Coord. Chem. Rev.* **2014**, *269*, 13-31.
[21] B. Weber, in *Spin-Crossover Materials*, John Wiley & Sons Ltd, **2013**, pp. 55-76.
[22] A. Real, J. Zarembowitch, O. Kahn, X. Solans, *Inorg. Chem.* **1987**, *26*, 2939-2943.
[23] S. Zein, S. A. Borshch, *J. Am. Chem. Soc.* **2005**, *127*, 16197-16201.
[24] R. Kulmaczewski, J. Olguín, J. A. Kitchen, H. L. C. Feltham, G. N. L. Jameson, J. L. Tallon, S. Brooker, *J. Am. Chem. Soc.* **2014**, *136*, 878-881.
[25] E. D. Doidge, J. W. Roebuck, M. R. Healy, P. A. Tasker, *Coord. Chem. Rev.* **2015**, *288*, 98-117.
[26] J. J. A. Kolnaar, M. I. d. Heer, H. Kooijman, A. L. Spek, G. Schmitt, V. Ksenofontov, P. Gütlich, J. G. Haasnoot, J. Reedijk, *Eur. J. Inorg. Chem.* **1999**, *1999*, 881-886.
[27] Y. Garcia, F. Robert, A. D. Naik, G. Zhou, B. Tinant, K. Robeyns, S. Michotte, L. Piraux, *J. Am. Chem. Soc.* **2011**, *133*, 15850-15853.
[28] O. Roubeau, P. Gamez, S. J. Teat, *Eur. J. Inorg. Chem.* **2013**, *2013*, 934-942.
[29] B. Ding, Y. Y. Liu, Y. Wang, J.-G. Ma, Z. Niu, W. Shi, P. Cheng, *Inorg. Chem. Commun.* **2013**, *31*, 44-48.
[30] X. X. Wu, Y. Y. Wang, P. Yang, Y. Y. Xu, J. Z. Huo, B. Ding, Y. Wang, X. Wang, *Cryst. Growth Des.* **2014**, *14*, 477-490.
[31] X. Cheng, Q. Yang, C. Gao, B.-W. Wang, T. Shiga, H. Oshio, Z.-M. Wang, S. Gao, *Dalton Trans.* **2015**, *44*, 11282-11285.

[32] B. A. Leita, B. Moubaraki, K. S. Murray, J. P. Smith, J. D. Cashion, *Chem. Commun.* **2004**, 156-157.
[33] K. Nakano, N. Suemura, S. Kawata, A. Fuyuhiro, T. Yagi, S. Nasu, S. Morimoto, S. Kaizaki, *Dalton Trans.* **2004**, 982-988.
[34] K. Nakano, S. Kawata, K. Yoneda, A. Fuyuhiro, T. Yagi, S. Nasu, S. Morimoto, S. Kaizaki, *Chem. Commun.* **2004**, 2892-2893.
[35] K. Nakano, N. Suemura, K. Yoneda, S. Kawata, S. Kaizaki, *Dalton Trans.* **2005**, 740-743.
[36] C. J. Schneider, J. D. Cashion, B. Moubaraki, S. M. Neville, S. R. Batten, D. R. Turner, K. S. Murray, *Polyhedron* **2007**, *26*, 1764-1772.
[37] M. Sy, F. Varret, K. Boukheddaden, G. Bouchez, J. Marrot, S. Kawata, S. Kaizaki, *Angew. Chem. Int. Ed.* **2014**, *53*, 7539-7542.
[38] C. J. Schneider, J. D. Cashion, N. F. Chilton, C. Etrillard, M. Fuentealba, J. A. K. Howard, J.-F. Létard, C. Milsmann, B. Moubaraki, H. A. Sparkes, S. R. Batten, K. S. Murray, *Eur. J. Inorg. Chem.* **2013**, *2013*, 850-864.
[39] S. Rodríguez-Jiménez, H. L. C. Feltham, S. Brooker, *Angew. Chem. Int. Ed.* **2016**, *55*, 15067-15071.
[40] J. S. Costa, S. Rodriguez-Jimenez, G. A. Craig, B. Barth, C. M. Beavers, S. J. Teat, G. Aromi, *J. Am. Chem. Soc.* **2014**, *136*, 3869-3874.
[41] J. A. Kitchen, N. G. White, G. N. L. Jameson, J. L. Tallon, S. Brooker, *Inorg. Chem.* **2011**, *50*, 4586-4597.
[42] J. A. Kitchen, J. Olguín, R. Kulmaczewski, N. G. White, V. A. Milway, G. N. L. Jameson, J. L. Tallon, S. Brooker, *Inorg. Chem.* **2013**, *52*, 11185-11199.
[43] R. W. Hogue, H. L. C. Feltham, R. G. Miller, S. Brooker, *Inorg. Chem.* **2016**, *55*, 4152-4165.
[44] C. F. Herold, S. I. Shylin, E. Rentschler, *Inorg. Chem.* **2016**, *55*, 6414-6419.
[45] C. Köhler, E. Rentschler, *Eur. J. Inorg. Chem.* **2016**, *2016*, 1955-1960.
[46] R. W. Saalfrank, H. Maid, A. Scheurer, *Angew. Chem., Int. Ed.* **2008**, *47*, 8794-8824.
[47] C. Piguet, G. Bernardinelli, G. Hopfgartner, *Chem. Rev.* **1997**, *97*, 2005-2062.
[48] F. Tuna, M. R. Lees, G. J. Clarkson, M. J. Hannon, *Chem., Eur. J.* **2004**, *10*, 5737-5750.
[49] D. Pelleteret, R. Clerac, C. Mathoniere, E. Harte, W. Schmitt, P. E. Kruger, *Chem. Commun.* **2009**, 221-223.
[50] N. Struch, J. G. Brandenburg, G. Schnakenburg, N. Wagner, J. Beck, S. Grimme, A. Lützen, *Eur. J. Inorg. Chem.* **2015**, *2015*, 5503-5510.
[51] C. S. Hawes, C. M. Fitchett, P. E. Kruger, *Supramol. Chem.* **2012**, *24*, 553-562.
[52] H. Hagiwara, T. Tanaka, S. Hora, *Dalton Trans.* **2016**, *45*, 17132-17140.
[53] H. Phan, J. J. Hrudka, D. Igimbayeva, L. M. Lawson Daku, M. Shatruk, *J. Am. Chem. Soc.* **2017**, *139*, 6437-6447.
[54] M. Darawsheh, L. A. Barrios, O. Roubeau, S. J. Teat, G. Aromí, *Chem., Eur. J.* **2016**, *22*, 8635-8645.
[55] M. D. Darawsheh, L. A. Barrios, O. Roubeau, S. J. Teat, G. Aromí, *Chem. Commun.* **2017**, *53*, 569-572.
[56] H. Takezawa, T. Murase, G. Resnati, P. Metrangolo, M. Fujita, *Angew. Chem. Int. Ed.* **2015**, *54*, 8411-8414.
[57] B. Icli, E. Solari, B. Kilbas, R. Scopelliti, K. Severin, *Chem., Eur. J.* **2012**, *18*, 14867-14874.
[58] B. K. Roland, H. D. Selby, M. D. Carducci, Z. Zheng, *J. Am. Chem. Soc.* **2002**, *124*, 3222-3223.
[59] D. Aguila, L. A. Barrios, O. Roubeau, S. J. Teat, G. Aromi, *Chem. Commun.* **2011**, *47*, 707-709.
[60] D. Fedaoui, Y. Bouhadja, A. Kaiba, P. Guionneau, J.-F. Létard, P. Rosa, *Eur. J. Inorg. Chem.* **2008**, *2008*, 1022-1026.
[61] A. Y. Verat, N. Ould-Moussa, E. Jeanneau, B. Le Guennic, A. Bousseksou, S. A. Borshch, G. S. Matouzenko, *Chem., Eur. J.* **2009**, *15*, 10070-10082.
[62] K. Dankhoff, C. Lochenie, F. Puchtler, B. Weber, *Eur. J. Inorg. Chem.* **2016**, *2016*, 2136-2143.
[63] G. S. Matouzenko, E. Jeanneau, A. Yu. Verat, A. Bousseksou, *Dalton Trans.* **2011**, *40*, 9608-9618.

[64] G. S. Matouzenko, E. Jeanneau, A. Y. Verat, Y. de Gaetano, *Eur. J. Inorg. Chem.* **2012**, *2012*, 969-977.
[65] Y. de Gaetano, E. Jeanneau, A. Y. Verat, L. Rechignat, A. Bousseksou, G. S. Matouzenko, *Eur. J. Inorg. Chem.* **2013**, *2013*, 1015-1023.
[66] J. J. M. Amoore, C. J. Kepert, J. D. Cashion, B. Moubaraki, S. M. Neville, K. S. Murray, *Chem., Eur. J.* **2006**, *12*, 8220-8227.
[67] J. J. M. Amoore, S. M. Neville, B. Moubaraki, S. S. Iremonger, K. S. Murray, J.-F. Létard, C. J. Kepert, *Chem., Eur. J.* **2010**, *16*, 1973-1982.
[68] M. Quesada, P. de Hoog, P. Gamez, O. Roubeau, G. Aromi, B. Donnadieu, C. Massera, M. Lutz, A. L. Spek, J. Reedijk, *Eur. J. Inorg. Chem.* **2006**, *2006*, 1353-1361.
[69] S. Kanegawa, S. Kang, O. Sato, *Eur. J. Inorg. Chem.* **2013**, *2013*, 725-729.
[70] W. A. Gobeze, V. A. Milway, J. Olguín, G. N. L. Jameson, S. Brooker, *Inorg. Chem.* **2012**, *51*, 9056-9065.
[71] E. Milin, S. Belaïd, V. Patinec, S. Triki, G. Chastanet, M. Marchivie, *Inorg. Chem.* **2016**, *55*, 9038-9046.
[72] J. G. Park, I.-R. Jeon, T. D. Harris, *Inorg. Chem.* **2015**, *54*, 359-369.
[73] M. van der Meer, Y. Rechkemmer, F. D. Breitgoff, R. Marx, P. Neugebauer, U. Frank, J. van Slageren, B. Sarkar, *Inorg. Chem.* **2016**, *55*, 11944-11953.
[74] D. Savard, C. Cook, G. D. Enright, I. Korobkov, T. J. Burchell, M. Murugesu, *CrystEngComm* **2011**, *13*, 5190-5197.
[75] G. Vos, R. A. G. De Graaff, J. G. Haasnoot, A. M. Van der Kraan, P. De Vaal, J. Reedijk, *Inorg. Chem.* **1984**, *23*, 2905-2910.
[76] G. Vos, R. A. Le Febre, R. A. G. De Graaff, J. G. Haasnoot, J. Reedijk, *J. Am. Chem. Soc.* **1983**, *105*, 1682-1683.
[77] V. Gomez, J. Benet-Buchholz, E. Martin, J. R. Galan-Mascaros, *Chem., Eur. J.* **2014**, *20*, 5369-5379.
[78] V. Gomez, C. S. de Pipaon, P. Maldonado-Illescas, J. C. Waerenborgh, E. Martin, J. Benet-Buchholz, J. R. Galan-Mascaros, *J. Am. Chem. Soc.* **2015**, *137*, 11924-11927.
[79] B. Schneider, S. Demeshko, S. Dechert, F. Meyer, *Angew. Chem. Int. Ed.* **2010**, *49*, 9274-9277.
[80] M. Steinert, B. Schneider, S. Dechert, S. Demeshko, F. Meyer, *Angew. Chem., Int. Ed.* **2014**, *53*, 6135-6139.
[81] J. Cirera, *Rev. Inorg. Chem.* **2014**, *34*, 199-216.
[82] A. Bousseksou, G. Molnar, L. Salmon, W. Nicolazzi, *Chem. Soc. Rev.* **2011**, *40*, 3313-3335.
[83] P. Gutlich, *Eur. J. Inorg. Chem.* **2013**, *2013*, 581-591.
[84] O. Kahn, C. J. Martinez, *Science* **1998**, *279*, 44-48.
[85] C. Bartual-Murgui, E. Natividad, O. Roubeau, *J. Mater. Chem. C* **2015**, *3*, 7916-7924.
[86] A. Grosjean, N. Daro, S. Pechev, L. Moulet, C. Etrillard, G. Chastanet, P. Guionneau, *Eur. J. Inorg. Chem.* **2016**, *2016*, 1961-1966.
[87] A. Urakawa, W. Van Beek, M. Monrabal-Capilla, J. R. Galan-Mascaros, L. Palin, M. Milanesio, *J. Phys. Chem. C* **2011**, *115*, 1323-1329.
[88] C. M. Quintero, G. Felix, I. Suleimanov, J. S. Costa, G. Molnar, L. Salmon, W. Nicolazzi, A. Bousseksou, *Beilstein J. Nanotechnol.* **2014**, *5*, 2230-2239.
[89] Y. X. Wang, D. Qiu, S. F. Xi, Z. D. Ding, Z. J. Li, Y. X. Li, X. H. Ren, Z. G. Gu, *Chem. Commun.* **2016**, *52*, 8034-8037.
[90] J. Dugay, M. Gimenez-Marques, T. Kozlova, H. W. Zandbergen, E. Coronado, H. S. J. van der Zant, *Adv. Mater.* **2015**, *27*, 1288-1293.
[91] J. R. Galán-Mascarós, E. Coronado, A. Forment-Aliaga, M. Monrabal-Capilla, E. Pinilla-Cienfuegos, M. Ceolin, *Inorg. Chem.* **2010**, *49*, 5706-5714.
[92] J. M. Herrera, S. Titos-Padilla, S. J. A. Pope, I. Berlanga, F. Zamora, J. J. Delgado, K. V. Kamenev, X. Wang, A. Prescimone, E. K. Brechin, E. Colacio, *J. Mater. Chem. C* **2015**, *3*, 7819-7829.
[93] Y. S. Koo, J. R. Galan-Mascaros, *Adv. Mater.* **2014**, *26*, 6785-6789.
[94] S. Rat, V. Nagy, I. Suleimanov, G. Molnar, L. Salmon, P. Demont, L. Csoka, A. Bousseksou, *Chem. Commun.* **2016**, *52*, 11267-11269.
[95] H. J. Shepherd, I. A. Gural'skiy, C. M. Quintero, S. Tricard, L. Salmon, G. Molnar, A. Bousseksou, *Nature Commun.* **2013**, *4*.

[96] I. A. Gural'skiy, V. A. Reshetnikov, A. Szebesczyk, E. Gumienna-Kontecka, A. I. Marynin, S. I. Shylin, V. Ksenofontov, I. O. Fritsky, *J. Mater. Chem. C* **2015**, *3*, 4737-4741.
[97] I. A. Gural'skiy, O. I. Kucheriv, S. I. Shylin, V. Ksenofontov, R. A. Polunin, I. O. Fritsky, *Chem., Eur. J.* **2015**, *21*, 18076-18079.
[98] I. Braunlich, S. Lienemann, C. Mair, P. Smith, W. Caseri, *J. Mater. Sci.* **2015**, *50*, 2355-2364.
[99] M. M. Dirtu, F. Schmit, A. D. Naik, I. Rusu, A. Rotaru, S. Rackwitz, J. A. Wolny, V. Schunemann, L. Spinu, Y. Garcia, *Chem., Eur. J.* **2015**, *21*, 5843-5855.
[100] M. M. Dîrtu, A. D. Naik, A. Rotaru, L. Spinu, D. Poelman, Y. Garcia, *Inorg. Chem.* **2016**, *55*, 4278-4295.
[101] C. M. Jureschi, J. Linares, A. Rotaru, M. H. Ritti, M. Parlier, M. M. Dirtu, M. Wolff, Y. Garcia, *Sensors* **2015**, *15*, 2388-2398.
[102] N. R. de Tacconi, K. Rajeshwar, R. O. Lezna, *Chem. Mater.* **2003**, *15*, 3046-3062.
[103] D. Li, R. Clérac, O. Roubeau, E. Harté, C. Mathonière, R. Le Bris, S. M. Holmes, *J. Am. Chem. Soc.* **2008**, *130*, 252-258.
[104] V. Niel, J. M. Martinez-Agudo, M. C. Muñoz, A. B. Gaspar, J. A. Real, *Inorg. Chem.* **2001**, *40*, 3838-3839.
[105] M. Ohba, K. Yoneda, G. Agusti, M. C. Munoz, A. B. Gaspar, J. A. Real, M. Yamasaki, H. Ando, Y. Nakao, S. Sakaki, S. Kitagawa, *Angew. Chem., Int. Ed.* **2009**, *48*, 4767-4771.
[106] C. H. Pham, J. Cirera, F. Paesani, *J. Am. Chem. Soc.* **2016**, *138*, 6123-6126.
[107] G. Félix, M. Mikolasek, H. Peng, W. Nicolazzi, G. Molnár, A. I. Chumakov, L. Salmon, A. Bousseksou, *Phys. Rev. B* **2015**, *91*, 024422.
[108] H. N. Peng, S. Tricard, G. Felix, G. Molnar, W. Nicolazzi, L. Salmon, A. Bousseksou, *Angew. Chem., Int. Ed.* **2014**, *53*, 10894-10898.
[109] D. M. Sagar, F. G. Baddour, P. Konold, J. Ullom, D. A. Ruddy, J. C. Johnson, R. Jimenez, *J. Phys. Chem. Lett.* **2016**, *7*, 148-153.
[110] S. Bonhommeau, G. Molnar, A. Galet, A. Zwick, J. A. Real, J. J. McGarvey, A. Bousseksou, *Angew. Chem., Int. Ed.* **2005**, *44*, 4069-4073.
[111] M. Castro, O. Roubeau, L. Piñeiro-López, J. A. Real, J. A. Rodríguez-Velamazán, *The Journal of Physical Chemistry C* **2015**, *119*, 17334-17343.
[112] S. Cobo, D. Ostrovskii, S. Bonhommeau, L. Vendier, G. Molnár, L. Salmon, K. Tanaka, A. Bousseksou, *J. Am. Chem. Soc.* **2008**, *130*, 9019-9024.
[113] J. E. Clements, J. R. Price, S. M. Neville, C. J. Kepert, *Angew. Chem., Int. Ed.* **2016**, *55*, 15105-15109.
[114] J. E. Clements, J. R. Price, S. M. Neville, C. J. Kepert, *Angew. Chem., Int. Ed.* **2014**, *53*, 10164-10168.
[115] M. Paez-Espejo, M. Sy, K. Boukheddaden, *J. Am. Chem. Soc.* **2016**, *138*, 3202-3210.
[116] N. F. Sciortino, K. R. Scherl-Gruenwald, G. Chastanet, G. J. Halder, K. W. Chapman, J. F. Letard, C. J. Kepert, *Angew. Chem., Int. Ed.* **2012**, *51*, 10154-10158.
[117] I. A. Gural'skiy, B. O. Golub, S. I. Shylin, V. Ksenofontov, H. J. Shepherd, P. R. Raithby, W. Tremel, I. O. Fritsky, *Eur. J. Inorg. Chem.* **2016**, 3191-3195.
[118] V. Niel, M. C. Munoz, A. B. Gaspar, A. Galet, G. Levchenko, J. A. Real, *Chem., Eur. J.* **2002**, *8*, 2446-2453.
[119] I. A. Gural'skiy, S. I. Shylin, B. O. Golub, V. Ksenofontov, I. O. Fritsky, W. Tremel, *New J. Chem.* **2016**, *40*, 9012-9016.
[120] J. Y. Li, Y. C. Chen, Z. M. Zhang, W. Liu, Z. P. Ni, M. L. Tong, *Chem., Eur. J.* **2015**, *21*, 1645-1651.
[121] J.-Y. Li, Z.-P. Ni, Z. Yan, Z.-M. Zhang, Y.-C. Chen, W. Liu, M.-L. Tong, *CrystEngComm* **2014**, *16*, 6444-6449.
[122] Z.-P. Ni, J.-L. Liu, M. N. Hoque, W. Liu, J.-Y. Li, Y.-C. Chen, M.-L. Tong, *Coord. Chem. Rev.* **2017**, *335*, 28-43.
[123] X. Bao, H. J. Shepherd, L. Salmon, G. Molnar, M. L. Tong, A. Bousseksou, *Angew. Chem., Int. Ed.* **2013**, *52*, 1198-1202.
[124] R. Ohtani, M. Arai, A. Hori, M. Takata, S. Kitao, M. Seto, S. Kitagawa, M. Ohba, *J. Inorg. Organomet. Polym. Mater.* **2013**, *23*, 104-110.
[125] J.-Y. Li, C.-T. He, Y.-C. Chen, Z.-M. Zhang, W. Liu, Z.-P. Ni, M.-L. Tong, *J. Mater. Chem. C* **2015**, *3*, 7830-7835.

[126] K. Yoshida, D. Akahoshi, T. Kawasaki, T. Saito, T. Kitazawa, *Polyhedron* **2013**, *66*, 252-256.
[127] K. Hosoya, S.-i. Nishikiori, M. Takahashi, T. Kitazawa, *Magnetochemistry* **2016**, *2*, 8.
[128] Z. Arcís-Castillo, M. C. Muñoz, G. Molnár, A. Bousseksou, J. A. Real, *Chem., Eur. J.* **2013**, *19*, 6851-6861.
[129] L. Piñeiro-López, Z. Arcís-Castillo, M. C. Muñoz, J. A. Real, *Cryst. Growth Des.* **2014**, *14*, 6311-6319.
[130] F. J. Muñoz-Lara, A. B. Gaspar, M. C. Muñoz, V. Ksenofontov, J. A. Real, *Inorg. Chem.* **2013**, *52*, 3-5.
[131] F. J. Muñoz-Lara, Z. Arcís-Castillo, M. C. Muñoz, J. A. Rodríguez-Velamazán, A. B. Gaspar, J. A. Real, *Inorg. Chem.* **2012**, *51*, 11126-11132.
[132] F. J. Valverde-Muñoz, M. Seredyuk, M. C. Muñoz, K. Znovjyak, I. O. Fritsky, J. A. Real, *Inorg. Chem.* **2016**, *55*, 10654-10665.
[133] J. Okabayashi, S. Ueno, Y. Wakisaka, T. Kitazawa, *Inorg. Chim. Acta* **2015**, *426*, 142-145.
[134] T. Kitazawa, Y. Gomi, M. Takahashi, M. Takeda, M. Enomoto, A. Miyazaki, T. Enoki, *J. Mater. Chem.* **1996**, *6*, 119-121.
[135] O. I. Kucheriv, S. I. Shylin, V. Ksenofontov, S. Dechert, M. Haukka, I. O. Fritsky, I. y. A. Gural'skiy, *Inorg. Chem.* **2016**, *55*, 4906-4914.
[136] W. Liu, L. Wang, Y.-J. Su, Y.-C. Chen, J. Tucek, R. Zboril, Z.-P. Ni, M.-L. Tong, *Inorg. Chem.* **2015**, *54*, 8711-8716.
[137] J. Okabayashi, S. Ueno, T. Kawasaki, T. Kitazawa, *Inorg. Chim. Acta* **2016**, *445*, 17-21.
[138] T. Kosone, T. Kitazawa, *Inorg. Chim. Acta* **2016**, *439*, 159-163.
[139] E. Milin, V. Patinec, S. Triki, E.-E. Bendeif, S. Pillet, M. Marchivie, G. Chastanet, K. Boukheddaden, *Inorg. Chem.* **2016**, *55*, 11652-11661.
[140] N. F. Sciortino, F. Ragon, K. A. Zenere, P. D. Southon, G. J. Halder, K. W. Chapman, L. Piñeiro-López, J. A. Real, C. J. Kepert, S. M. Neville, *Inorg. Chem.* **2016**, *55*, 10490-10498.
[141] S.-L. Zhang, X.-H. Zhao, Y.-M. Wang, D. Shao, X.-Y. Wang, *Dalton Trans.* **2015**, *44*, 9682-9690.
[142] R. Herchel, Z. Trávníček, R. Zbořil, *Inorg. Chim. Acta* **2011**, *365*, 458-461.
[143] F. Setifi, C. Charles, S. Houille, F. Thétiot, S. Triki, C. J. Gómez-García, S. Pillet, *Polyhedron* **2013**, *61*, 242-247.
[144] S.-i. Ohkoshi, K. Imoto, Y. Tsunobuchi, S. Takano, H. Tokoro, *Nat Chem* **2011**, *3*, 564-569.
[145] D. Pinkowicz, M. Rams, M. Mišek, K. V. Kamenev, H. Tomkowiak, A. Katrusiak, B. Sieklucka, *J. Am. Chem. Soc.* **2015**, *137*, 8795-8802.
[146] R.-M. Wei, M. Kong, F. Cao, J. Li, T.-C. Pu, L. Yang, X.-L. Zhang, Y. Song, *Dalton Trans.* **2016**, *45*, 18643-18652.
[147] E. Coronado, M. Giménez-Marqués, G. Mínguez Espallargas, F. Rey, I. J. Vitórica-Yrezábal, *J. Am. Chem. Soc.* **2013**, *135*, 15986-15989.
[148] N. Calvo Galve, E. Coronado, M. Giménez-Marqués, G. Mínguez Espallargas, *Inorg. Chem.* **2014**, *53*, 4482-4490.
[149] M. Weselski, M. Książek, J. Kusz, A. Białońska, D. Paliwoda, M. Hanfland, M. F. Rudolf, Z. Ciunik, R. Bronisz, *Eur. J. Inorg. Chem.* **2017**, *2017*, 1171-1179.
[150] A. Białońska, R. Bronisz, J. Kusz, M. Zubko, *Eur. J. Inorg. Chem.* **2013**, *2013*, 884-893.
[151] M. Seredyuk, L. Piñeiro-López, M. C. Muñoz, F. J. Martínez-Casado, G. Molnár, J. A. Rodriguez-Velamazán, A. Bousseksou, J. A. Real, *Inorg. Chem.* **2015**, *54*, 7424-7432.
[152] M. Ksiazek, J. Kusz, A. Bialonska, R. Bronisz, M. Weselski, *Dalton Trans.* **2015**, *44*, 18563-18575.
[153] J.-B. Lin, W. Xue, B.-Y. Wang, J. Tao, W.-X. Zhang, J.-P. Zhang, X.-M. Chen, *Inorg. Chem.* **2012**, *51*, 9423-9430.
[154] Y.-C. Chuang, C.-T. Liu, C.-F. Sheu, W.-L. Ho, G.-H. Lee, C.-C. Wang, Y. Wang, *Inorg. Chem.* **2012**, *51*, 4663-4671.
[155] W. Liu, X. Bao, J.-Y. Li, Y.-L. Qin, Y.-C. Chen, Z.-P. Ni, M.-L. Tong, *Inorg. Chem.* **2015**, *54*, 3006-3011.
[156] X. Bao, P.-H. Guo, W. Liu, J. Tucek, W.-X. Zhang, J.-D. Leng, X.-M. Chen, I. y. Gural'skiy, L. Salmon, A. Bousseksou, M.-L. Tong, *Chem. Sci.* **2012**, *3*, 1629-1633.
[157] F.-L. Yang, M.-G. Chen, X.-L. Li, J. Tao, R.-B. Huang, L.-S. Zheng, *Eur. J. Inorg. Chem.* **2013**, *2013*, 4234-4242.

[158] X.-R. Wu, H.-Y. Shi, R.-J. Wei, J. Li, L.-S. Zheng, J. Tao, *Inorg. Chem.* **2015**, *54*, 3773-3780.
[159] Y.-H. Luo, Q.-L. Liu, L.-J. Yang, Y. Ling, W. Wang, B.-W. Sun, *J. Solid State Chem.* **2015**, *222*, 76-83.
[160] J. A. Real, E. Andrés, M. C. Muñoz, M. Julve, T. Granier, A. Bousseksou, F. Varret, *Science* **1995**, *268*, 265-267.
[161] T. Romero-Morcillo, N. De la Pinta, L. M. Callejo, L. Piñeiro-López, M. C. Muñoz, G. Madariaga, S. Ferrer, T. Breczewski, R. Cortés, J. A. Real, *Chem., Eur. J.* **2015**, *21*, 12112-12120.
[162] C. Göbel, T. Palamarciuc, C. Lochenie, B. Weber, *Chem., Asian J.* **2014**, *9*, 2232-2238.
[163] O. Klimm, C. Gobel, S. Rosenfeldt, F. Puchtler, N. Miyajima, K. Marquardt, M. Drechsler, J. Breu, S. Forster, B. Weber, *Nanoscale* **2016**, *8*, 19058-19065.
[164] F. Shao, J. Li, J.-P. Tong, J. Zhang, M.-G. Chen, Z. Zheng, R.-B. Huang, L.-S. Zheng, J. Tao, *Chem. Commun.* **2013**, *49*, 10730-10732.
[165] T. Romero-Morcillo, F. J. Valverde-Munoz, M. C. Munoz, J. M. Herrera, E. Colacio, J. A. Real, *RSC Adv.* **2015**, *5*, 69782-69789.
[166] A. Lennartson, P. Southon, N. F. Sciortino, C. J. Kepert, C. Frandsen, S. Mørup, S. Piligkos, C. J. McKenzie, *Chem., Eur. J.* **2015**, *21*, 16066-16072.
[167] S. Schonfeld, C. Lochenie, P. Thoma, B. Weber, *CrystEngComm* **2015**, *17*, 5389-5395.
[168] H.-Y. Wang, J.-Y. Ge, C. Hua, C.-Q. Jiao, Y. Wu, C. F. Leong, D. M. D'Alessandro, T. Liu, J.-L. Zuo, *Angew. Chem. Int. Ed.* **2017**, *56*, 5465-5470.
[169] R. Ohtani, K. Shimayama, A. Mishima, M. Ohba, R. Ishikawa, S. Kawata, M. Nakamura, L. F. Lindoy, S. Hayami, *J. Mater. Chem. C* **2015**, *3*, 7865-7869.
[170] K. Bhar, S. Khan, J. S. Costa, J. Ribas, O. Roubeau, P. Mitra, B. K. Ghosh, *Angew. Chem. Int. Ed.* **2012**, *51*, 2142-2145.
[171] S. Roy, S. Choubey, K. Bhar, N. Sikdar, J. S. Costa, P. Mitra, B. K. Ghosh, *Dalton Trans.* **2015**, *44*, 7774-7776.